ABSTRACTS

ANNUAL PROJECT CONFERENCE

JULY 2023

TECHNION
Israel Institute of Technology

BME Faculty of Biomedical Engineering
TECHNION - Israel Institute of Technology

Dear all,

We are proud and honored to welcome you to take part in the: ***Annual Project Presentation Conference 2023 of the Biomedical Engineering Faculty***.

This meeting culminates a yearlong research and development experience of our 4th year students. There is a say in Hebrew tradition: "אין חכם כבעל ניסיון", meaning "Experience brings wisdom". This in a nut shell, is what the projects are all about.

During their project development experience, our students had to undergo through all the stages needed to make an idea come true. Starting with a medical problem which they had to tackle, they had to strain their imagination and think "out of the box" in order to come up with a plausible new solution. Then, they had to combine the knowledge they gained during their studies. This knowledge encompasses all the aspects of biomedical engineering, i.e. combining medical background with engineering skills and scientific knowledge. All this package had to be implemented in order to provide a real world solution.

We believe that this hands-on experience exposed and prepared our graduates to the High-Tech biomedical industry and to a wide variety of biomedical research in a very strong way encouraging multidisciplinary work that is vital for the students' future career, and in addition potentially foster their entrepreneurship skills.

In this booklet the abstracts of all presented projects are displayed for your perusal. We are sure that the students are eager to present the outcome of their year-long projects. We wish all of them rewarding careers after graduation. We hope that very soon they will take an active part in similar projects as professional mentors from both the industry and academia.

Kindest Regards,

Prof. Haim Azhari, Faculty Dean

Dr. Firas Mawase, Course Instructor

List of abstracts

1. Noninvasive Optoacoustic Mapping of Local Oxygen Concentration in The Inflamed Bone Marrow Niche

Ruth Pikovsky[1], Shirly Hagay[1], Ashish Tiwari [1], Liron McLey[1], Katrien Vandoorne[1]
[1] Faculty of Biomedical Engineering, Technion - IIT, Haifa, Israel

2. Automatic Placental Defects Detection System

Tikva Moravia[1], Maor Granot[1], Dana Vinter[2], Rotem Shapira[1], Yaakov Diminsky[3]
[1] Faculty of Biomedical Engineering, Technion - IIT, Haifa, Israel
[2] Rambam Hospital
[3] Road2 Haifa

3. Deep Learning Model for Endoscopic CRS Endotypic Classification Using Preoperative Diagnostic Nasal Endoscopy Images

Kamar Dawahdi[1], Nofe Jawamees [1], Dr. Tamar Tobi Porat [2], and Agmon Porat [3]
[1] Faculty of Biomedical Engineering, Technion - IIT, Haifa, Israel
[2] Department of Otolaryngology – The Baruch Padeh Medical Center, Poriya, Israel
[3] Kencap Ltd, Yehud, Israel

4. Silicon Nanowires Fabrication and Photoelectrochemical Performance Optimization

Alon Remer[1], Philip Borochov[1], Nadi Hathot[1] and Menahem Y. Rotenberg[1]
[1] Faculty of Biomedical Engineering, Technion - IIT, Haifa, Israel

5. Complexity Measures in Brain Activity of Schizophrenic Patients

Roee Mey-Tal[1], Arin Twito[1], Rotem Shapira[1], and Avi Peled[2,3]
[1] Faculty of Biomedical Engineering, Technion - IIT, Haifa, Israel
[2] Ma'ale HaCarmel Mental Health Center, Tirat Carmel, Israel
[3] Rappaport Faculty of Medicine, Technion - IIT, Haifa, Israel

6. Evaluation of solid-state nanopores temporal resolution for DNA Translocations

Zohar Rosenstock[1], Omer Talmon[1], Neeraj Soni[2], and Amit Meller[3]
[1] Faculty of Biomedical Engineering, Technion - IIT, Haifa, Israel

7. Quantifiable Methods in Silicon Nanowires Cellular Uptake

Yasmin Habib[1], Lara Mbarki[1], Tania Assaf[1], Merav Belenkovich[1], Oryan Karni[1] and Hemi (Menahem) Rotenberg[1]
[1]Faculty of Biomedical Engineering, Technion - IIT, Haifa, Israel

8. Simulating Agent Behavior Using Reinforcement Learning

Ofer Drori[1], Nir Sassy[1], Ben Engelhard[2]
[1] Faculty of Biomedical Engineering, Technion - IIT, Haifa, Israel
[2] Faculty of Medicine, Engelhard Lab, Technion - IIT, Haifa, Israel

9. 3D Reconstruction and Analysis of Hydra Regeneration in Lightsheet Microscopy
Yoad Goldfaden[1], Yonit Maroudas-Sacks[2], Lital Shani-Zerbib[2], Iris Pasvinter[2], Gaia Levin[3] and Kinneret Keren[2]
[1] Faculty of Biomedical Engineering, Technion - IIT, Haifa, Israel
[2] Kinneret Keren's Experimental Biophysics Lab, Faculty of Physics, IIT, Haifa, Israel
[3] Yoav Schectman's Nano-bio Optics Lab, Faculty of Biomedical Engineering, IIT, Haifa, Israel

10. Bone Marrow Endothelial Changes During Diabetes Mellitus
Siraj Nsraldeen[1], Nedaa Kher[1], Narmeen Haj[1], Katrien Vandoorne[1]
[1]Faculty of Biomedical Engineering, Technion - IIT, Haifa, Israel

11. Head Phantom
Lena Elias[1], Kanar Asakli[1], Gil Isschar[2], and Rotem Shapira[1]
[1] Faculty of Biomedical Engineering, Technion - IIT, Haifa, Israel
[2] Firefly Neuroscience, Hod Hasharon, Israel

12. Enhancing accessibility with an adaptive keyboard application and mechanical support for people with disabilities
Fadi Jeries[1], Shada Kardosh[1], Gaia Levin[2] and Firas Mawase[3]
[1] Faculty of Biomedical Engineering, Technion - IIT, Haifa, Israel
[2] Nano-bio-optics Lab, Faculty of Biomedical Engineering, Technion, IIT, Haifa, Israel
[3] Mawase Lab, Faculty of Biomedical Engineering, Technion, IIT, Haifa, Israel

13. Design Of a Platform Used To Measure The Effect Of Antiarrhythmic Drugs On Pluripotent Stem Cell-derived Cardiomyocytes (hiPSC-CMs)
Rotem Solomon[1], Anat Rotschield[1], Savyon Mazgaoker[1], Oryan Karni[2], Merav Belenkovich[3] and Yael Yaniv[1]
[1] Laboratory of Bioelectric and Bioenergetic Systems, Faculty of Biomedical Engineering, Technion - IIT, Haifa, Israel
[2] Laboratory of Stem Cell and Tissue Engineering, Faculty of Biomedical Engineering, Technion
[3] Laboratory of Cardiovascular Nano-Med Engineering, Faculty of Biomedical Engineering, Technion - IIT, Haifa, Israel

14. Use of Speech Analysis for the Assessment of Depression and Cognitive Impairment in Elderly People
Shir Singer[1], Maya Goldshalger[1], Daniel Harlev[2], Eyal Bergmann[2]
[1] Faculty of Biomedical Engineering, Technion - IIT, Haifa, Israel.
[2] Psychiatric Division, Department of Psychiatry, Rambam Medical Center, Haifa, Israel.

15. Deep-learning-based Registration for Hippocampal Atrophy Detection in aging and Alzheimer's disease
Habib Azzam[1], Yazan Nasser[1], Samah Khawaled [2], Gaia Levin[1], Moti Freiman[1]
[1] Faculty of Biomedical Engineering, Technion - IIT, Haifa, Israel
[2] Faculty of Applied Mathematics, Technion - IIT, Haifa, Israel

16. Differentiating reading gains in children with attention deficit hyperactivity disorder and children with reading difficulties objectively using fMRI data and machine learning
Masa Khashab, Sanad Ghanaiem, Tzipi Horowitz-Kraus, Rula Farah
[1] Faculty of Biomedical Engineering, Technion - IIT, Haifa, Israel
[2] Faculty of Education in Science and Technology - IIT, Haifa, Israel

17. Chronic obstructive pulmonary disease diagnosis from oximetry time series
Shir Hadad[1], Hadar Cohen[1], Jeremy Levy[1]
[1] Faculty of Biomedical Engineering, Technion - IIT, Haifa, Israel

18. DNA Origami Structure for Improving Gene Editing by CRISPR/Cas9
Dana Gal[1], Ronnie Itzhaki[1], Hadas Omer[1], Gaia Levin[1], and Yuval Garini[1]
[1] Faculty of Biomedical Engineering, Technion - IIT, Haifa, Israel

19. Electrostatic Effects on Inhaled Aerosol Deposition in the Lung Bronchi
Morane Elbaze[1], Leo Ibghi[1], Ron Bessler[1], and Josué Sznitman[1]
[1] Faculty of Biomedical Engineering, Technion - IIT, Haifa, Israel

20. Predicting Clinical Response to Radiotherapy Treatment in CRC Patients
Bashar Khoury[1], Jeries Saleh[1], Yinon Goldstein[2], Noam Keidar[1], Yonatan Elul[2] and Assaf Schuster[2]
[1] Faculty of Biomedical Engineering, Technion - IIT, Haifa, Israel
[2] Faculty of Computer Science, Technion - IIT, Haifa, Israel

21. Phantom-Based Characterization of Human Skin Tissue and Blood Vessels for Preliminary In-Vitro Blood Count Experiments
Oshri Hemo Ferraro[1], Tal Darbinovski[1], Reut Friedman[2], and Dvir Yelin[2]
[1] Faculty of Biomedical Engineering, Technion - IIT, Haifa, Israel
[2] Faculty of Biomedical Engineering, Biomedical Optics Lab, Technion - IIT, Haifa, Israel

22. Cancer cells as a drug delivery system for Osteosarcoma
Maya Naim[1], Roy Meretzki[1], Orr Bar Natan[1,2], and Yosi Shamay[1]
[1] Faculty of Biomedical Engineering, Technion - IIT, Haifa, Israel
[2] Nanomedicine and Nanotechnology Interdisciplinary Program, Technion - IIT, Haifa, Israel

23. Video-Based Lie Detection: Unveiling Truth through Heart Rate Variability
Shir Eitan[1], Inbar bar[1], Ido Weiser-Bitoun[1], Moran Davoodi[1], and Yael Yaniv[1]
[1]Faculty of Biomedical Engineering, Technion - IIT, Haifa, Israel

24. Diffusion Model Simulator
Maia Lehrman[1], Tav Nahimov[1], Alon Saguy[1], Gaia Levin[1], Yoav Shechtman[1]
[1]Faculty of Biomedical Engineering, Technion - IIT, Haifa, Israel

25. Quantification of diabetic infarct healing with multimodal imaging using optomagnetic nanoparticles

Noa Levi[1], Maya Sharoni[1], Betsalel Elgrably[1], and Katrien Vandoorne[1]
[1] Faculty of Biomedical Engineering, Technion - IIT, Haifa, Israel

26. Fetal EEG: New Born Babies EEG Artifact cleaning and features

Fatma Ebraheem[1], Fauzi Jomaa[1], Zhuo Wang[2], Rotem Shapira[1], and Offer Erez[3]
[1] Faculty of Biomedical Engineering, Technion – ITT, Haifa, Israel
[2] Drexel University School of Biomedical Engineering, Science and Health care
[3] Ben-Gurion University the Joyce and Irving Goldman Medical School

27. Cancer Cells Detection in Spectral-Imaged Biopsies using Machine Learning

Chen Ziv [1], Daniela Boguslavsky [1], Adam Soker [1] and Yuval Garini [1]
[1] Faculty of Biomedical Engineering, Technion - IIT, Haifa, Israel

28. Effects of Microplastic on Alginate Hydrogel Mechanics as a Model for Tissues

Noga Drimer Hocherman[1], Tamar Gil[1], Baptiste Le Roi[2], Merav Belenkovich[1], Oryan Karni Katovich[1], Joshua Grolman[2]
[1]Faculty of Biomedical Engineering, Technion – ITT, Haifa, Israel
[2]Faculty of Materials Engineering, Technion – ITT, Haifa, Israel

29. Dynamic Reinforcement Learning Enabled by Virtual Reality

Irina Shkalikov[1], Tamar Ben yaacov[1], Ben Engelhard [2]
[1] Faculty of Biomedical Engineering, Technion - IIT, Haifa, Israel
[2] Engelhard Lab Neural circuits for complex behavior

30. Decreased Frontal Theta Frequency While Performing a Task with the Existence of Smartphone Among Children: An EEG Study

Rawnaq Shaer[1], Sheherban Nasser Eldin[1], Carmel Gashri[1], Gaia Levin[1], Tzipi Horowitz-Kraus[2]
[1]Faculty of Biomedical Engineering, Technion - IIT, Haifa, Israel
[2]Faculty of Education in Science and Technology – IIT, Haifa, Israel

31. Developing a Non-Invasive Imaging Platforms to Genetically Track Hematopoietic Stem and Progenitor Cells and Their Offspring During Inflammation

Mira Waked[1], Liron-Hanan Waingerten-Kedem[1], Shiri Ashkenazi[1], Katrien Vandoorne[1]
[1]Faculty of Biomedical Engineering, Technion - IIT, Haifa, Israel

32. Reducing the electrocardiogram time series lead system for arrhythmia diagnosis and age estimation tasks

Shahar Rashty[1], Sarah Teitz[1], Rotem Shapira[1], Eran Zvuloni[1] and Joachim Behar[1]
[1] Faculty of Biomedical Engineering, Technion - IIT, Haifa, Israel

1

Noninvasive Optoacoustic Mapping of Local Oxygen Concentration in The Inflamed Bone Marrow Niche

Ruth Pikovsky[1], Shirly Hagay[1], Ashish Tiwari [1], Liron McLey[1], Katrien Vandoorne[1]

[1] Faculty of Biomedical Engineering, Technion - IIT, Haifa, Israel

Introduction: Inflammation triggers hematopoietic stem cell proliferation in the bone marrow niche, generating a cellular inflammatory response. When stem cells in the bone marrow proliferate to produce inflammatory cells, we hypothesize that they consume more oxygen due to higher metabolic demands. Optoacoustic imaging is a noninvasive, ionizing radiation free, label-free, in vivo imaging technique that combines rich contrast of optical excitation and deep penetration of ultrasound detection. Intravascular oxygen saturation can be estimated through optoacoustic-based assessment of oxy- and deoxy-hemoglobin.
The goal of our project was to set up a novel, noninvasive imaging method to evaluate the hemoglobin oxygenation changes during inflammation in bone marrow blood vessels by optoacoustic imaging.

Methods: We first verified noninvasive imaging by comparing invasive optoacoustic imaging using a skin flap surgery with imaging while leaving the skin intact. We used two mice models of inflammation: we compared (1) healthy control mice, with (2) mice induced with acute inflammation by injection of lipopolysaccharide, and (3) mice injected with streptozotocin, inducing a type 1 diabetes therefore modelling chronic inflammation. After the experiment, blood was taken for complete blood count and mice were sacrificed. Femurs were isolated for histological analysis, and skulls isolated to verify localization of the bone marrow vessels imaged. MATLAB-based processing was used to reconstruct the real time acquired data using filtered back-projection and parameter tuning. Finally, spectral demixing was done to calculate the oxygenation and deoxygenation values of hemoglobin by choosing the region of interest in the mice skull and generating the oxy and deoxy parametric maps. For histology, the organs were placed into 4% paraformaldehyde overnight, embedded in paraffin and sectioned. After decalcification and embedding, samples were stained with H&E.

Results: To verify the location of the calvaria vessels, an axial histological section through the skull found only a very thin layer of the skull located above the vessels. Measurements and data processing led to mean oxygen values that were lower for the chronic inflammation model than the control. One-way ANOVA statistical analysis led to statistical significance between the chronic and the control groups. The acute group was not statistically significant compared to the other groups.
The total blood count revealed an increased number of neutrophils in the acute mice model and chronic mice model compared to controls.

Conclusions: The oxygen measurements were lower for the chronic inflammation model. The other measurements were consistent with these findings. Therefore, we conclude that multispectral optoacoustic imaging is an effective and reliant tool for the assessment of oxygen concentration and could revolutionize the diagnostic process of diseases symptomized with inflammation.

Keywords: Optoacoustic imaging, inflammation, oxygen concentration

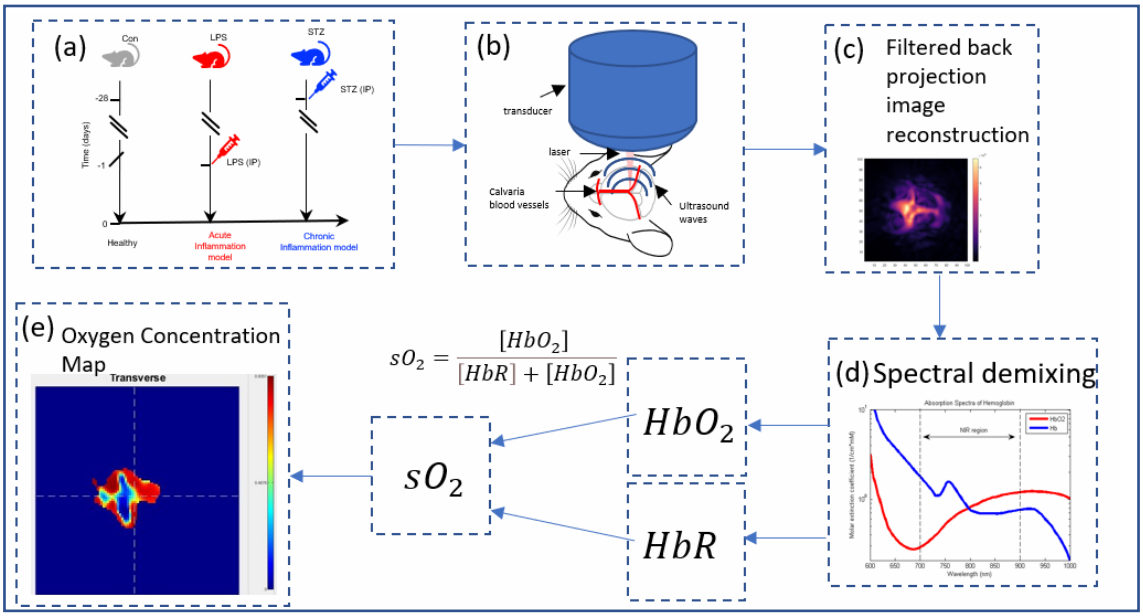

Figure 1: Schematic diagram of the experiment steps. (a) model preparation, (b) optoacoustic setup and measurement, (c) signal reconstruction, (d) spectral demixing to estimate oxyhemoglobin and deoxyhemoglobin concentration, (e) oxygen concentration map generation.

2

Automatic Placental Defects Detection System

Tikva Moravia[1], Maor Granot[1], Dana Vinter[2], Rotem Shapira[1], Yaakov Diminsky[3]

[1] Faculty of Biomedical Engineering, Technion - IIT, Haifa, Israel
[2] Rambam Hospital
[3] Road2 Haifa

Introduction:

The placenta is created early in pregnancy, It plays critical roles in facilitating nutrients, gas and waste exchange, protects from infections and acts as an endocrine organ producing hormones during pregnancy.

After a baby is born, most placentas are expelled from the uterus spontaneously. The placentas do not undergo a routine examination by a pathologist, only when it is considered necessary, and resources are available. The integrity of placenta is determined grossly by the staff (nurses, midwifes, obstetricians). In 3-6% of deliveries, there is placenta residue in the uterus, which may cause complications as severe as infection and secondary infertility. Therefore, when the placenta is suspected to be partially absent and a suspicion for retained products of conception (RPOC) in the uterus is risen, women undergo a manual exploration of uterus.

Despite that management, in some women, the placenta is being assessed mistakenly as complete, and later, it is discovered that the woman has RPOC that is known to be associated with immediate and delayed postpartum hemorrhage, infections, intrauterine adhesions, secondary infertility and pain.

Methods:

Our project methodology involved collaboration with medical and engineering teams. We held meetings with the medical staff to characterized the medical need. We consulted researchers in image processing and scanner technologies to identify the scanner technology that is the most suitable and procured relevant components. We met with patent agent to check the best tactic to protect the product. This comprehensive approach enabled us to develop an innovative solution to address the challenges in the field.

Results:

Selection of scanning technology- we thoroughly evaluated various options including photogrammetric scanning, lidar scanning, and structured light scanning. After careful consideration, we opted for a scanner utilizing Light Structured technology due to its ability to produce high-quality scans with excellent resolution at a relatively low cost.

In selecting the scanning device, we considered multiple factors including resolution, accuracy, price, focal distance, and well-documented software with a software development kit (SDK).

The availability of an SDK enabled seamless integration of the scanner into other software and provided flexibility in managing various scanning functions according to our specific needs.

The scanning device structure was chosen to ensure the preservation of the scanner, ease of operation, and a compact size.

The additional equipment selected for the scanning device includes a rotating plate, a weighing device and a barcode scanner.

Conclusions:

our project focused on characterizing a product designed to revolutionize the understanding of normal and damaged placentas by creating an extensive database. This invaluable resource empowers medical professionals to make informed decisions, ultimately reducing the incidence of misdiagnosis. Through close collaboration with interdisciplinary teams of engineers and doctors, we successfully identified the essential specifications for the measuring device, including scanning technology, resolution, accuracy, scanner size, and focal distance.

Keywords:

placenta, structured-light, Scanning

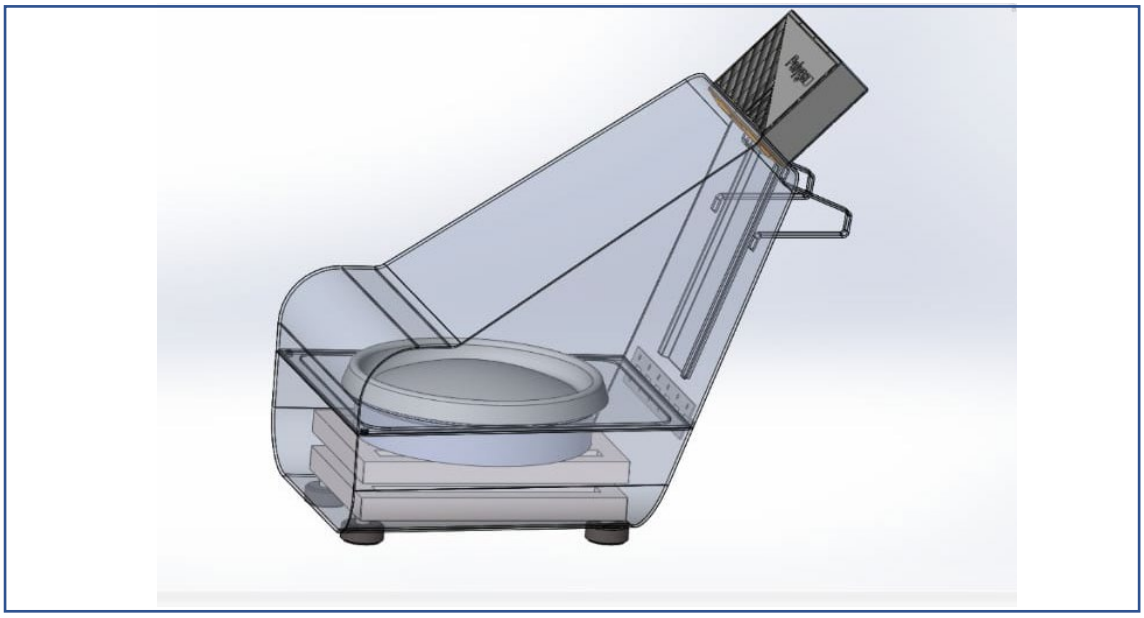

Figure 1: example of scanning facility

3

Deep Learning Model for Endoscopic CRS Endotypic Classification Using Preoperative Diagnostic Nasal Endoscopy Images

Kamar Dawahdi[1], Nofe Jawamees [1], Dr. Tamar Tobi Porat [2], and Agmon Porat [3]

1 Faculty of Biomedical Engineering, Technion - IIT, Haifa, Israel
2 Department of Otolaryngology – The Baruch Padeh Medical Center, Poriya, Israel
3 Kencap Ltd, Yehud, Israel

Introduction: Chronic Rhinosinusitis (CRS) is an inflammatory disease of the nasal cavity and paranasal sinuses, it is one of the most prevalent chronic diseases. CRS seriously affects the quality of life, its typical symptoms: headaches, respiratory obstruction and decreased sense of smell and taste. It can also lead to life-threatening situations.

Classically, subgroups of CRS were defined based on phenotypes. A major limitation of the traditional phenotypic classification is that it does not account for pathophysiological differences. The current approach proposes endotypic diagnosis which defines the inflammatory type allowing for better orientation of therapy, this approach differentiate between eosinophilic and non-eosinophilic inflammatory responses. A definitive diagnosis of ECRS versus non-ECRS can be achieved through histopathological examination of sinonasal mucosa; however, it is invasive. Furthermore, given the high postoperative recurrence rate of ECRS and differences in the surgical methods for both CRS types, methods for accurate preoperative differentiation of the CRS type are needed. Diagnostic nasal endoscopy does not effectively distinguish ECRS from NECRS.

Considering the strong feature extraction and screening ability of artificial intelligence, applying artificial intelligence technology to diagnostic nasal endoscopy may allow preoperative differentiation between ECRS and NECRS.

Convolutional neural networks (CNN) are models based on deep neural learning (a form of AI), with multiple levels of data representation. A CNN has a high potential for feature extraction and analysis.

The objective of this study is to investigate the ability of deep learning-based models for detecting and classifying eosinophilic and non-eosinophilic CRS on preoperative transnasal endoscopic images.

Methods: A total of 53 chronic rhinosinusitis (CRS) patients undergoing nasal endoscopic surgery were included. Endoscopic images were pre-processed and used to build the dataset. Patients in each category were divided into training and validation groups at a ratio of 4:1 respectively. Augmentation to the training set was done to enlarge the data set we used common

pre-trained classification networks including EfficientNet-B0, Resnet_v1_50, Inception and MobileNet neural networks. These networks were trained using the Adam optimizer.

Results: We incorporated confusion matrices for class-wise comparison to analyze models reliability of classification. Resnet_v1_50 network showed the best performance with 77% accuracy, 70% precision and 82% F1 Score. Other networks showed 38-70% accuracy.

Conclusions: Deep learning models specifically CNN could effectively distinguish between ECRS and NECRS based on preoperative nasal endoscopic images. Diagnosis based AI improves physician accuracy, resulting in a better therapy orientation.

Keywords: endoscopy; deep learning; classification; CNN; chronic rhinosinusitis.

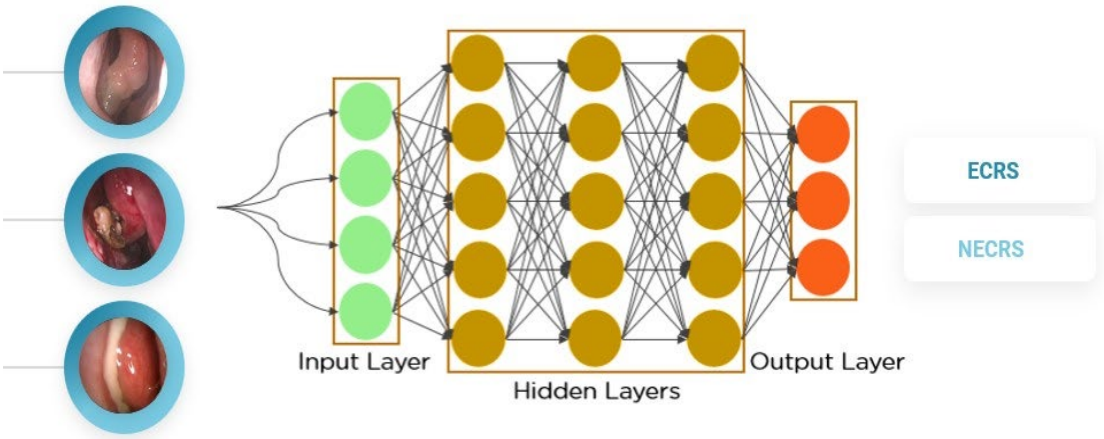

Figure 1: Convolutional Neural Network is a Deep Learning algorithm that can get input images, assign weights and biases to objects in the image, and be able to differentiate and classify these images.

4

Silicon Nanowires Fabrication and Photoelectrochemical Performance Optimization

Alon Remer[1], Philip Borochov[1], Nadi Hathot[1] and Menahem Y. Rotenberg[1]

[1] Faculty of Biomedical Engineering, Technion - IIT, Haifa, Israel

Introduction: The study of bioelectricity is crucial for understanding cellular behaviors, but most methods so far are invasive and interfere with the natural environment of the cell. Leadless biomodulation techniques like optogenetics offer solutions to those restrictions but lack spatial resolution and require genetic modification. Silicon nanowires are nanostructures that can be used as a bioelectrical interface and can be internalized by cells, thereby enabling local optical bioelectric modulation with submicron resolution. However, existing designs using photodiode configurations require complex fabrication that leads to non-uniform nanowires. We propose an alternative design based on nanoporous/non-porous semiconductor heterojunction, that was shown to exhibit a stronger photoelectrochemical response and a more deformable biointerface due to the porosity. This alternative approach allows for a simpler fabrication process that can be more precisely controlled. Our objective is to optimize this process and the photoelectrochemical properties of this design.

Methods: Silicon nanowires were fabricated from silicon wafers in a multi-stage process. P-type silicon wafers were used, and surface treated to enhance its hydrophilicity, in order to optimize the deposition of Polystyrene nanospheres (PS NSs) on it. A spin coater was utilized to deposit them on the wafer to obtain a monolayer and to maximize the coverage area. Scanning Electron Microscope (SEM) was used to examine samples throughout the entire process. In clean rooms, wafer surface underwent oxygen treatment to decrease the nanospheres' diameter. These nanospheres serve as masks, preventing etching of the wafer at their specific locations during either metal assisted chemical etching (MACE) or deep reactive ion etching (DRIE). Following the fabrication of the nanowires, they were treated with Hydrofluoric acid and Nitric acid to form a porous layer. SEM was employed to measure their lengths, diameters, and depth of the porous layer. The resulting nanowires and wafers were examined for their photoelectrical response by subjecting them to LED pulses of varying wavelengths and intensities using a patch clamp technique.

Results: We managed to fabricate silicon nanowires which demonstrated a unique pattern of photoelectrical response. Through various optimization processes, we were able to achieve an optimal MACE solution yielding a reasonable length of cylindrical nanowires. DRIE yielded good results as well, but the nanowires got a saw-like shape. Different ratios of porosity etching solutions affected both the layer depth and the performance under photoelectrical stimulation.

Conclusions: We have shown preliminary results to prove the feasibility of using silicon nanowires composed of nanoporous and non-porous layers to get a photoelectrical response

and further utilizing them in biomodulation of cells. Future work should fine tune the process to achieve a fully defined "recipe" for silicon nanowires.

Keywords: Semiconductors, Biomodulation, Silicon Nanowires, Etching, Photoelectronics.

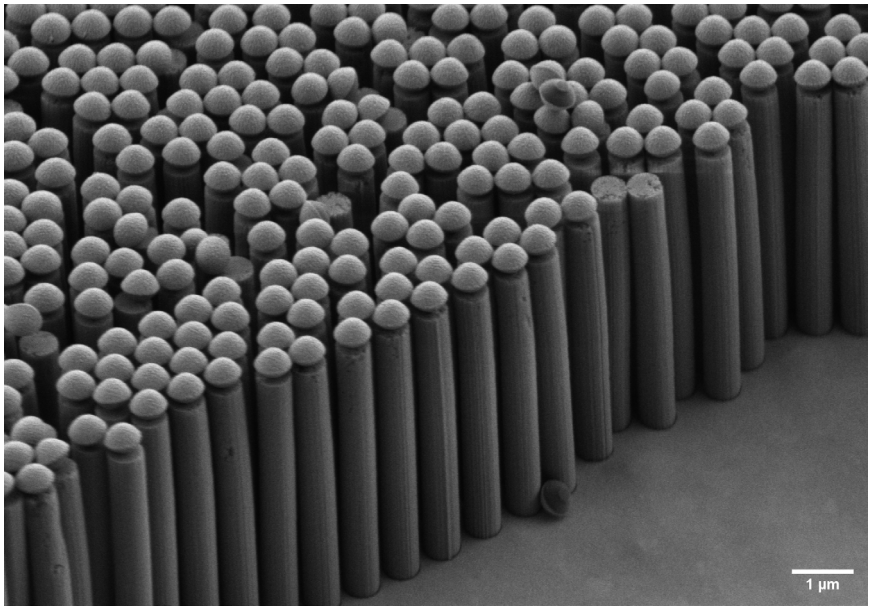

Figure 1: SEM image of fabricated Silicon Nanowires using metal assisted chemical etching.

5

Complexity Measures in Brain Activity of Schizophrenic Patients

Roee Mey-Tal[1], Arin Twito[1], Rotem Shapira[1], and Avi Peled[2,3]

[1] Faculty of Biomedical Engineering, Technion - IIT, Haifa, Israel
[2] Ma'ale HaCarmel Mental Health Center, Tirat Carmel, Israel
[3] Rappaport Faculty of Medicine, Technion -IIT, Haifa, Israel

Introduction:

Schizophrenia is a lifelong mental disorder characterized by several abnormalities, divided into positive and negative symptoms, in addition to cognitive deficiency. Diagnosis is based on assessing those symptoms, defined by the Diagnostic and Statistical Manual of Mental Disorders (DSM), in a form of interview being done by psychiatrist. However, since psychotic disorders are heterogeneous and might have overlapping features, the assessment may be inaccurate. Another challenge is the lack of knowledge regarding the causes of Schizophrenia, resulting in limited treatment. Therefore, a precise and objective diagnosis tool is needed.

Here, we will examine brain complexity measures applied on brain signals, Electroencephalogram (EEG) and Magnetoencephalography (MEG), as a potential biomarker. Relying on the leading theory that mental disorders characterized by disorganization of global brain networks, we aim to find a significant difference in the complexity values during different phases of the disorder, as well as between different groups of schizophrenic and healthy patients.

Methods:

EEG signals were sampled from 19 schizophrenic patients, in addition to matching psychiatric evaluation and medication records. MEG signals were sampled from 164 subjects, 100 healthy and 64 schizophrenics. Three different complexity measures were applied to both types of signals: Arrow of Time (AOT), Permutation Entropy (PE) and Lempel-Ziv Complexity (LZC). In order to find the correlation between the complexity value and the patient's state, an analysis of the relation between the symptoms and the results of the algorithms was made. In addition, statistical tests were applied on the MEG's results.

Results:

No correlation was found between the EEG signals' complexity and the schizophrenic subject state of the disease.

Results of the MEG whose complexity was calculated using the PE algorithm showed a clear difference between the healthy and schizophrenic groups. However, no significant differences were found between the MEG results that their complexities were quantified by AOT and LZC algorithms.

Conclusions:

In this research, we explored a thesis about the relation between brain signals' complexity and schizophrenia disease. We studied the given data with algorithms that were adapted especially for this project. Even though EEG signals did not show a correlation, MEG analysis showed an interesting result which matched our expectations. This unique result needs to be explored further, and emphasis should be placed on MEG recordings permutation entropy analysis of schizophrenic subjects during different states of the disease.

Keywords: Schizophrenia, Complexity, EEG, MEG

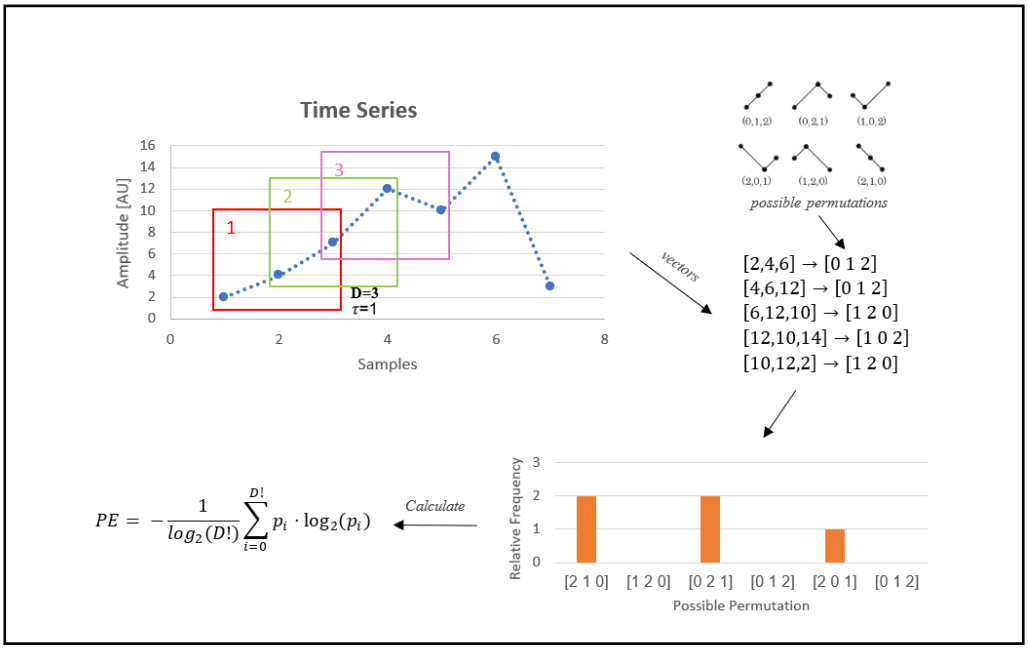

Figure 1: Schematic description of Permutation Entropy algorithm.
The ordinal patterns in the series are mapped into the possible permutations, which relative frequencies are used to compute the PE.

6

Evaluation of solid-state nanopores temporal resolution for DNA Translocations

Zohar Rosenstock[1], Omer Talmon[1], Neeraj Soni[2], and Amit Meller[3]

[1] Faculty of Biomedical Engineering, Technion - IIT, Haifa, Israel

Polymerase Chain Reaction (PCR) is a widely utilized enzymatic method for amplifying genome copies. It involves a nonlinear amplification process, where DNA is multiplied in cycles to achieve gene expression amplification for measurement purposes. However, quantifying gene expression can be complicated due to variations in the threshold cycle. Additionally, this amplification process can result in variations in the streak of amplified genome, leading to the possibility of false-negative and false-positive test outcomes. Although certain approaches, such as electrophoretic separation of nucleic acid fragments on a gel, have improved speed, cost, and complexity, there is still room for further advancements in these areas.

Single-molecule sensing methods can bypass some limitations of amplification-based detection, provided that it offers sufficient specificity for DNA sensing. Nanopores are an emerging class of single-molecule biosensors, developed primarily for single-molecule DNA sequencing. These are the single-molecule aperture fabricated in an electrically insulating membrane that separates the two-buffer solution containing reservoirs, namely Cis and Trans. On applying the electric potential, a steady ionic flow occurs through the nanopore, constituting the open pore current (i_o). The transient blocked in the flow of ions by a biomolecule is called blocked current (i_b). These translocations are the interplay of the electrophoretic and electroosmotic flow. The throughput of the method is the rate at which molecules arrive and thread into the pores. Thanks to their high sensitivity, and their relatively low-cost, nanopores have been adapted as biosensors for sensing DNA and proteins, specifically, solid-state nanopores (ssNPs).

To date, however, the use of ssNP for quantitative molecular detection has limited separation power between DNA populations discriminated by length. We managed to drill a sub 5 nm stable pore and sense 100 bp DNA, and discriminate it from 400 bp DNA. The events were analyzed by dwell time and by current drop characteristics and built a two-dimensional GMM model where the events were separated into two populations. In previous experiment the populations separated was 400 bp DNA and 3000 bp DNA.

Based on the results, it can be deduced that longer DNA exhibit a higher degree of variation, which poses difficulties in effectively segregating long DNA into distinct populations. Attaining a resolution of 100 base pairs proves to be a challenging objective within the limitations of the experimental conditions, thus representing the maximum resolution achieved in this project. To surpass these limitations, it is advisable to conduct additional experiments

involving the creation of narrower pores. Moreover, future research may focus on investigating the separation of multiple (> 2) populations and exploring diverse types of biopolymers.

Keywords: Solid State Nanopores, DNA Sensing, Single Molecule, Nanopore Resolution

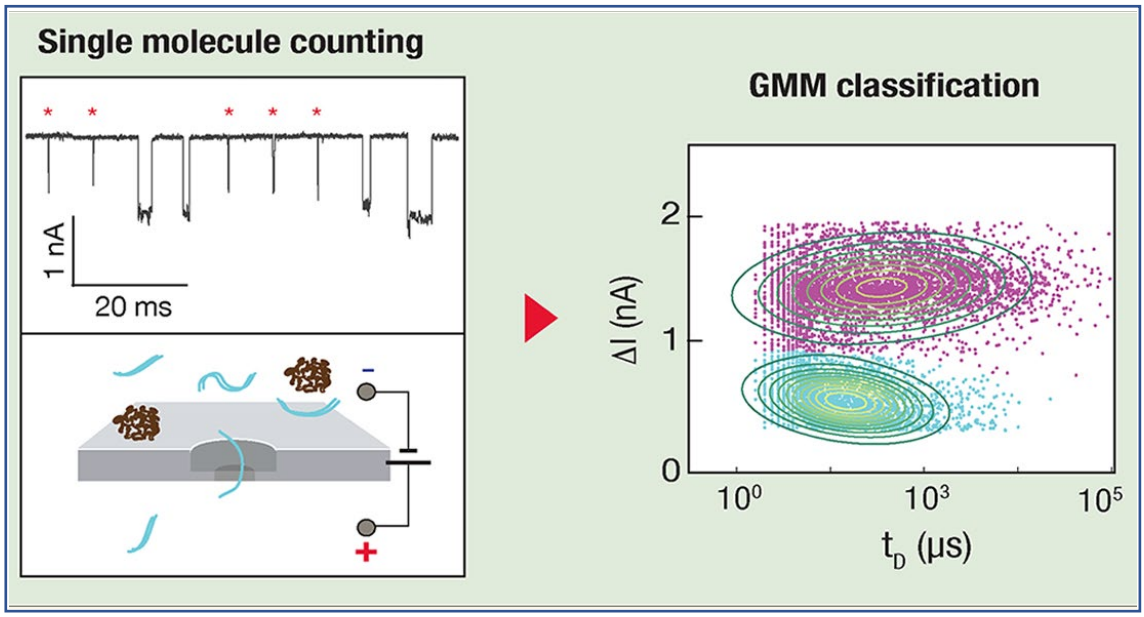

Figure 1: Single-molecule DNA expression analysis using nanopores. On the left an illustration of the pored membrane in the DNA aquatic solution and the events characteristic above it. On the right there is the GMM analysis of two separated populations.

7

Quantifiable Methods in Silicon Nanowires Cellular Uptake

Yasmin Habib[1], Lara Mbarki[1], Tania Assaf[1], Merav Belenkovich[1], Oryan Karni[1] and Hemi (Menahem) Rotenberg[1]

[1] Faculty of Biomedical Engineering, Technion - IIT, Haifa, Israel

Introduction: Intracellular bioelectric interrogation offers exciting opportunities for understanding cell biology and designing next-generation therapeutic devices. Currently, the most widely used methodologies in this field are bulky, substrate bound, harmful to cells, and might require genetic modifications, limiting their potential clinical applications. Moreover, they exhibit poor 3D spatial resolution. Overcoming the current limitations, silicon nanowires (SiNWs) offer an alternative method for intracellular interrogation. It is a semiconductor nanomaterial, fabricated to have a diode like configuration. It can be spontaneously internalized into different types of cells, maintaining cell integrity (fig. 1a). Following internalization, cell-SiNW hybrids can be photostimulated via photoelectric and photothermal mechanisms using a focused laser, achieving submicron resolution and allowing modulation of electrical signals in excitable cells.

Here, we develop a robust quantification tool for measuring SiNWs internalization into cells in 2D and 3D cultures, as there is no gold standard for this measurement. Moreover, we evaluate the effects of SiNWs types, surface properties (doping, porosity etc.) and morphology on their cellular uptake, aiming to obtain significant correlations between the two.

Methods: Our quantification algorithm was developed using MATLAB and ImageJ. The system input is z-stack images of cells seeded with SiNWs, fluorescently dyed, and scanned with a confocal microscope. The algorithm quantifies the level of SiNWs cellular uptake, normalized by a cell volume unit. For code validation, manual SiNWs quantification was conducted by multiple individuals, independently.

Proceeding to assess the effects of SiNWs factors on cell-SiNWs hybrids' behavior, we started with concentration effects. The experimental system consisted of gradually increasing concentrations of SiNWs, seeded on identical Normal Human Dermal Fibroblasts (NHDF) culture plates. Multiple frames were scanned from each plate aiming to increase statistical significance. Internalization levels were measured using our algorithm. As a follow-up experiment, cell viability was assessed.

As recent research revealed the superiority of porous SiNWs interface in generating sufficient photoelectrochemical response, an additional experimental system was designed to evaluate the effects of SiNWs surface porosity levels on cellular uptake, viability and photoelectrochemical response.

Results: Our algorithm output indicated a positive correlation between SiNWs concentration and cellular uptake; however, saturation was observed in high concentrations (fig. 1c). While no monotonic trend was observed in cellular viability, moderate variations were detected in medium to high concentrations. Regarding SiNWs surface porosity, minor alterations in cell viability were observed in different porosity levels. Furthermore, results showed higher cellular uptake and photoelectrochemical response in higher porosity levels. However experimental repetitions are required to reach statistical significance.

Conclusions: We have developed a foolproof quantification tool to measure cellular internalization in 2D and 3D cell cultures. We have established quantifiable correlations between SiNWs properties (i.e. porosity and concentration) and their impact on cells.

Keywords: silicon nanowires (SiNWs), cellular uptake, photostimulation, bioelectric interrogation.

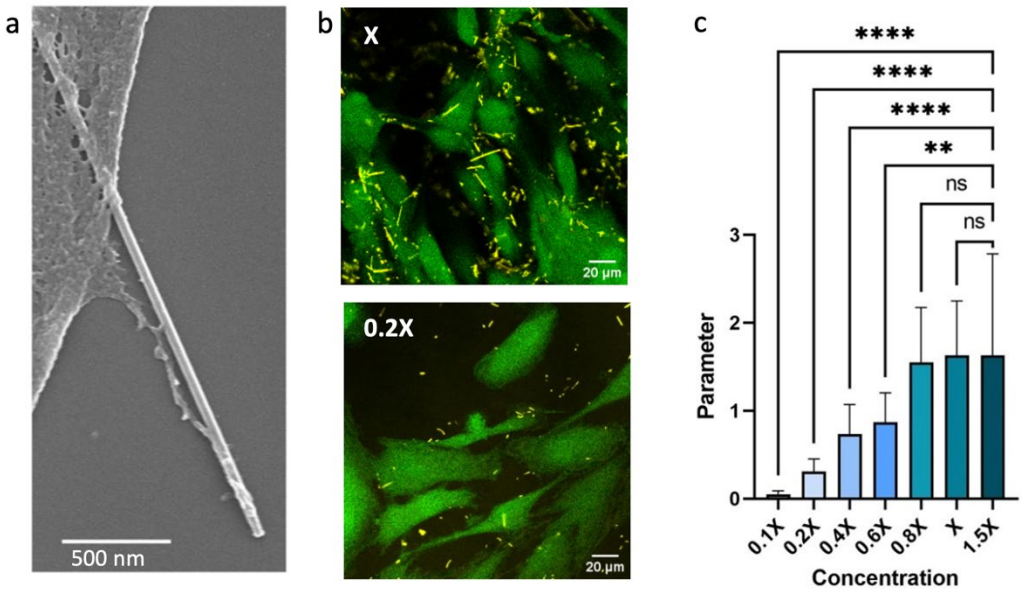

Fig. 1. (**a**) SEM micrograph showing membrane extension along a SiNW. (**b**) Confocal fluorescence image of NHDF cells (cytoplasm, green; SiNWs, yellow) with different SiNWs concentrations (x=24 fM). (**c**) uptake statistics of SiNWs with varying concentrations as measured by the algorithm (n=16).

8

Simulating Agent Behavior Using Reinforcement Learning

Ofer Drori[1], Nir Sassy[1], Ben Engelhard[2]

[1] Faculty of Biomedical Engineering, Technion - IIT, Haifa, Israel
[2] Faculty of Medicine, Engelhard Lab, Technion - IIT, Haifa, Israel

Introduction: Reinforcement learning (RL) is a subfield of machine learning (ML) that focuses on developing algorithms that enable agents to learn optimal behavior by interacting with their environment. Both RL and biological learning utilize reward signals as behavior guidelines. RL agents and biological learners receive feedback from the environment in the form of rewards or punishments, enabling the learner to understand which actions lead to positive outcomes. In ML, this feedback is commonly provided by assigning a reward signal for the agent's actions. In biological learning, the reward is provided by the release of neurotransmitters like dopamine in response to positive outcomes. According to the reward predicting error hypothesis, dopamine neurons encode the difference between expected reward and actual reward, also known as "Temporal Difference", a concept utilized in RL loss functions. RL and biological learning also involve the trade-off between known rewarding actions and exploring new actions that may yield greater rewards, referred to as the 'Exploration-Exploitation Trade-Off'. This has led to the belief that RL could be a fundamental mechanism in bio-learning methods. In this project we aim to extract learning signals from RL agents for comparison with biological learners.

Methods: **Deep Q-Learning Network (DQN)** is a value-based RL algorithm that learns a Q-function mapping state-action pairs to their values, representing the future cumulative reward. Using a deep neural network the algorithm approximates the Q-function by minimizing the temporal difference. **Proximal Policy Optimization (PPO)** is a policy-based 'Actor-Critic' RL algorithm used to approximate the policy, a function mapping states to actions. Using deep neural networks, the actor takes actions that try to maximize the critic's estimate, while the critic evaluates the actor's performance and updates its policy using the policy-gradient theorem. **PFRL** is a PyTorch-based open-source library that implements various state-of-the-art deep RL algorithms.

Results: Extracted learning signals from RL agents on complex tasks. Figure 1 displays the learning signals for the DQN agent on Atari's Breakout game. In addition, we established a platform for training and evaluating agents using various RL algorithms.

Conclusions: This project is part of a broader research that aims to understand biological learning through deep reinforcement learning and marks the first milestone in the process. Our extracted data will serve as a baseline for future comparisons with biological learners, and our platform enables easy conduction of further RL experiments in the lab if needed.

Keywords: Deep Reinforcement Learning, Machine Learning, Biological Learning.

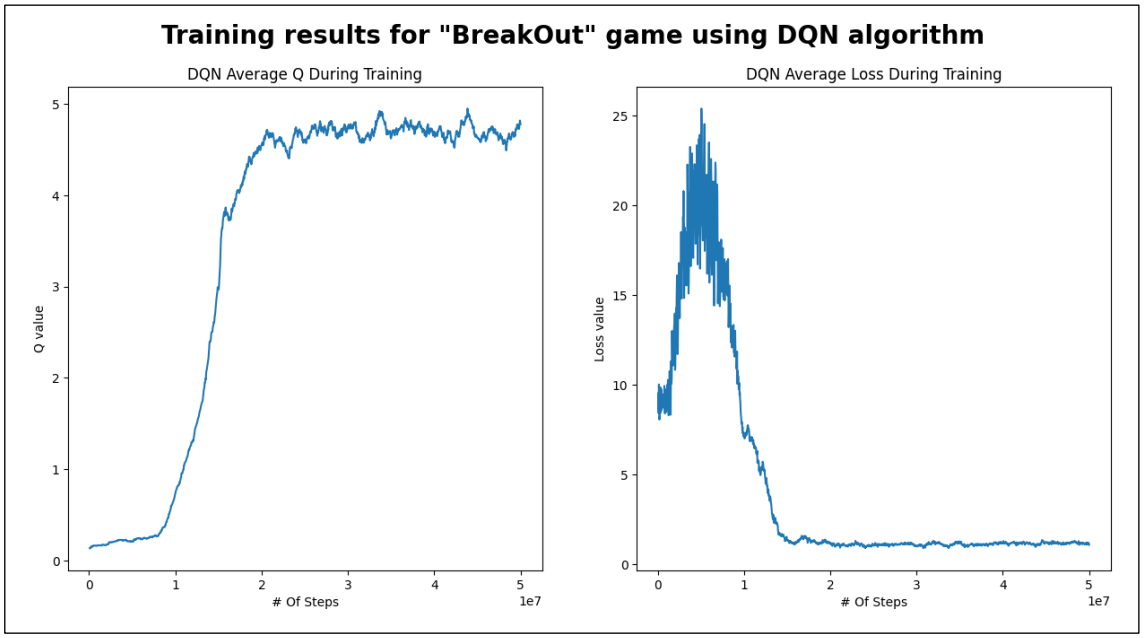

Figure 1: Learning curve for DQN algorithm. Average Q-values (left) and average loss (right) as function of the number of steps. Early rise in loss is a result of the agent's high exploration. It progressively shifts towards prioritizing exploitation, which leads to a decline in loss values and increase in Q-values.

9

3D Reconstruction and Analysis of Hydra Regeneration in Lightsheet Microscopy

Yoad Goldfaden[1], Yonit Maroudas-Sacks[2], Lital Shani-Zerbib[2], Iris Pasvinter[2], Gaia Levin[3] and Kinneret Keren[2]

[1] Faculty of Biomedical Engineering, Technion - IIT, Haifa, Israel
[2] Faculty of Physics, Kinneret Keren's Experimental Biophysics Lab
[3] Faculty of Biomedical Engineering, Yoav Schectman's Nano-bio Optics Lab

Introduction: Morphogenesis is the process of shaping and formation of organs and structures in living organisms. It includes the formation of the body plan, the development of organs, and the organization of tissues. The process of morphogenesis starts with the formation of a single cell (the zygote) and ends with the formation of a complex organism.

Kinneret's lab seeks to develop a conceptual understanding of the self-organizational principles that give rise to large-scale spatio-temporal patterns in living cells and multicellular animal. To this end, the lab utilizes Hydras, a freshwater predatory animal that is capable of full-body regeneration even from a small tissue piece. The process of regenerating the entire body is closely related to morphogenesis during embryogenesis.

The goal of this project is to create a tool that merge multiple lightsheet movies of regenerating hydras from various viewpoints into a single 3D representation. Automate and integrate it within the lab's data analysis environment and begin to perform in-depth image analysis and characterization of global spatial variables of the regenerative process in its entirety.

Methods: lightsheet fluorescence microscopy is a powerful imaging technique that allows for the high-resolution, three-dimensional imaging of living specimens at low-phototoxicity. It is particularly well suited for imaging large, transparent specimens such as embryos, organs and whole organisms.

Iterative Closest Point registration algorithm is a widely used method for aligning or registering point clouds, which are sets of 3D points representing an object or a scene. The algorithm iteratively minimizes the distance between the points in one point cloud and the closest points in the other point clouds, in order to find the optimal transformation (i.e. rotation and translation) that aligns the two or more point clouds.

Zen is a software platform designed for the acquisition and analysis of microscopy data, while ImageJ is a free, open-source software used for image analysis in scientific research. Both software provides a range of tools and functions for processing and analyzing images, making them popular choices for researchers in the scientific community.

Results and conclusions: A pipeline for generating 3D movies out of the raw microscope files was successfully developed and for the most part automated in such a way that even a new user without prior knowledge in imageJ could easily create 3D movies using this method.

Keywords: Lightsheet fluorescence microscopy, iterative closest point registration, ImageJ

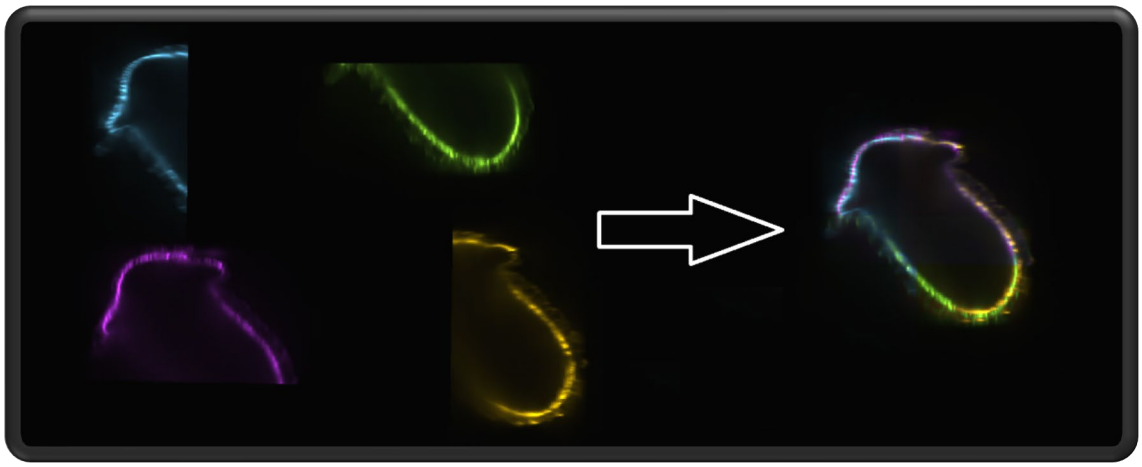

Figure 1: the beginning state and the result of the registration proccess.

10

Bone Marrow Endothelial Changes During Diabetes Mellitus

Siraj Nsraldeen[1], Nedaa Kher[1], Narmeen Haj[1], Katrien Vandoorne[1]

[1] Faculty of Biomedical Engineering, Technion - IIT, Haifa, Israel

Introduction: Diabetes mellitus is a chronic illness, described by metabolic disorders, characterized by hyperglycemia and defects in insulin secretion and/or insulin action. It is closely associated with the development of vascular complications in many vascular beds. Yet, diabetic changes to the bone marrow vasculature have not yet been described. Bone marrow vasculature is known in regulating the production and release of blood leukocytes, which protect the host against infection but also fuel inflammatory diseases. Inflammatory conditions are altered during diabetes and pose a very high risk of developing cardiovascular events, that could lead to heart failure and death.

In this project, we study the vascular changes in the diabetic bone marrow niche, where inflammatory cells are produced, which is still unknown. Moreover, how diabetes stimuli affect the bone marrow vasculature is poorly understood, which led us to conduct the study.

Methods: To verify bone marrow vessel sprouting, $Apln^{CreER}$; $Rosa26^{ZsGreen/+}$ reporter (Apln) mice, were either injected with STZ for 5 consecutive days to induce diabetes or served as age-matched control. All Apln mice, in which sprouting endothelial cells and their progeny express ZsGreen, were injected with tamoxifen. At 4 wks after STZ/tamoxifen injection, mice developed diabetes and were compared with only tamoxifen injected age-matched controls. Throughout the study, glucose levels and weight were monitored. Skull marrow of the mice were in vivo imaged using intravital confocal microscope to verify (1) $Apln^{+}$ sprouting vessels, (2) CD31+ vessels and (3) albumin-Cy5, as a blood pool agent that could quantify permeability. The images were analyzed using ImageJ software to quantify the newly formed blood vessels in the calvaria. After in vivo experiments, mice were sacrificed to isolate femurs. The femurs were shaved to expose the bone marrow and imaged using spinning disk confocal microscopy. Lastly, bone marrow of femurs from C57/Bl6 mice was isolated and endothelial bone marrow cells were stained ($Ter119^{-}CD41^{-}CD45^{-}CD31+Sca1^{+}$) for flow cytometry technique.

Results: In our study, intravital microscopic images of the bone marrow, 4 wks after induction of diabetes, showed an increase in new $Apln^{+}$ blood vessels as confirmed by quantification of the percentage area green fluorescence (Fig. A). Consistent with this, ex vivo microscopic images of the femoral bone marrow also showed increased expression of new blood vessels in diabetic mice. Furthermore, we initiated isolation of endothelial cells for flow cytometry and established a gating strategy to quantify endothelial cells for control and diabetic femoral bone marrow (Fig. B). These findings collectively indicate that diabetes is associated with enhanced blood vessel formation and higher levels of endothelial cells.

Conclusions: Our findings support the hypothesis that diabetes alters the bone marrow microenvironment, as we discovered that diabetes enhances angiogenesis in the bone marrow, which was validated by in vivo and ex vivo microscopy, as well as flow cytometry. This research promotes mechanistic understanding of the roots of diabetes and its inflammatory origins.

Keywords: diabetes, bone marrow, blood vessels, microscopy, flow cytometry

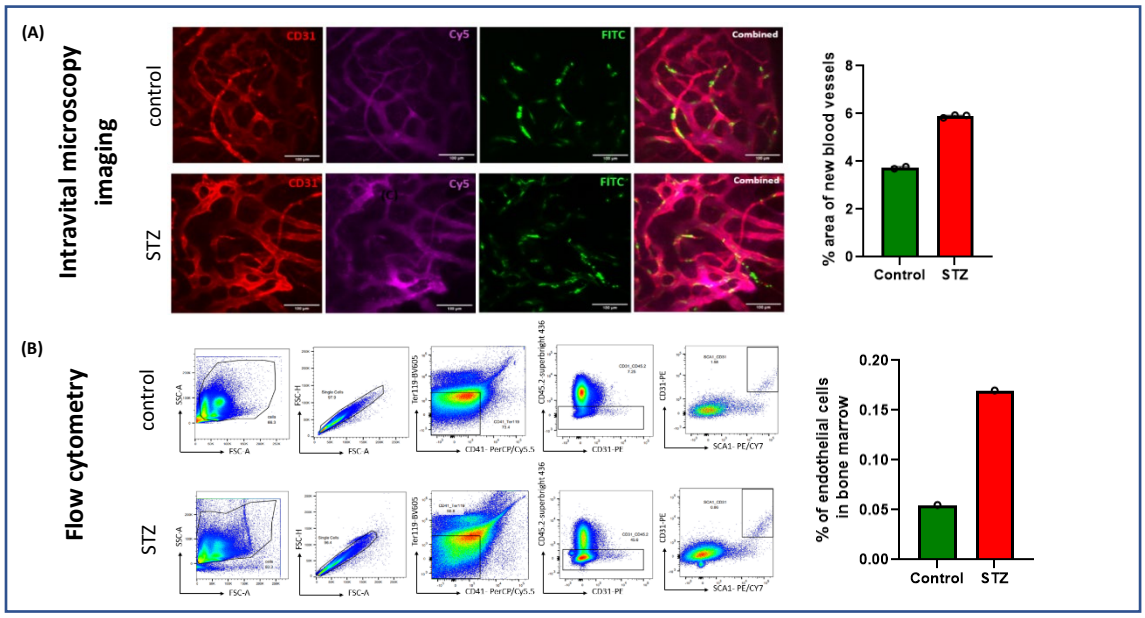

Figure: preliminary results showed increased bone marrow vasculature in diabetes. (A) Confocal images of blood vessels labeled with CD31, Cy5, FITC in Apln mice and quantification of blood vessels percentage area in control and STZ mice. (B) Flow cytometry gating strategy to identify endothelial cells through subgating for Sca1+ and CD31+ markers, and quantification of the endothelial cells percentage for both groups.

11

Head Phantom

Ms. Lena Elias[1], Ms. Kanar Asakli[1], Mr. Gil Isschar[2], and Ms. Rotem Shapira[3]

[1] Faculty of Biomedical Engineering, Technion - IIT, Haifa, Israel
[2] Firefly Neuroscience, Hod Hasharon, Israel
[3] Faculty of Biomedical Engineering, Technion - IIT, Haifa, Israel

Introduction: The EEG is a noninvasive procedure that measures the electrical activity of the brain using electrodes attached to the scalp. Brain cells constantly communicate through electrical impulses, which are represented as a wavy line in an EEG recording. However, when testing EEG systems on humans or animals, the results can be inconsistent and vary between tests due to factors such as the subject's current situation, emotions, and thought processes. As a result, the true electrophysiological signal being measured is unknown, making it challenging to validate these systems since there is no known "ground truth" signal available for comparison.

This study aims to build a head phantom that mimics the electrical properties of the scalp. This phantom will serve as a platform to attach electrodes and emit a pre-known signal. By doing so, it can be utilized to calibrate EEG systems effectively.

Method: To create an accurate EEG system testing phantom, the first step involved carefully selecting the components. Research and experimentation were conducted to identify materials with properties resembling electrical conductivity and impedance of the human scalp while taking factors such as dielectric properties, resistivity, elasticity, and frequency response in consideration in the selecting process.

The testing of the promising components involved a comparison with reference samples that were constructed based on literature, with the objective of achieving similar properties.

Additionally, AgCl EEG electrodes were chosen to ensure reliable signal transmission and reception. And two methods were used for measuring the impedance, first one is building an electrical circuit with multiple components (voltage meter, current meter, and signal generator), the second method for validation was SIGGI II by EasyCap (signal generator and impedance meter).

Following the selection of suitable components, we proceeded to perform validation tests on a promising component: a synthetic gelatin spray coated with metallic-based conductive paint.

Results: We obtained a promising sample of synthetic gelatin coated with metallic spray paint, exhibiting an impedance range of 0.2-0.6 kΩ. Although this impedance falls below the desired range of 1kΩ to 10kΩ, it is still suitable for calibrating EEG systems.

Conclusions: The errors that occurred can be attributed to inaccuracies during sample creation and changes in electrode positioning. Despite the impedance range being incorrect, the painted samples exhibited impedance values that closely resembled those of the reference samples.

Among the samples, one sample performed the best, with a thickness of 4cm, and it was the closest to the desired impedance range.

Keywords: EEG systems, Head Phantoms, Impedance, Electrical Properties.

Figure 1: Impedance measurement setup includes the following components: (a) SIGGI II by EasyCap as the measuring equipment, (b) Synthetic Gelatin Sample with Metallic Paint Coating, and (c) Three measuring electrodes.

12

Enhancing accessibility with an adaptive keyboard application and mechanical support for people with disabilities

Fadi Jeries[1], Shada Kardosh[1], Gaia Levin[2] and Firas Mwase[3]

[1] Faculty of Biomedical Engineering, Technion - IIT, Haifa, Israel
[2] Faculty of Biomedical Engineering, Technion, Nano-bio-optics Lab
[3] Faculty of Biomedical Engineering, Technion, Mawase Lab

Introduction: People with different disabilities can face numerous challenges in communicating, especially those with speech impairments. Communication skills are crucial for human development, particularly during their formative years, as well as for engaging in everyday activities. Many individuals experience both communication disabilities and motor impairments, which further compound their difficulties.

Existing solutions available today offer limited assistance, such as keyboard applications that enable communication through typing. However, these solutions are not effective in all cases, especially the most severe ones. One issue with existing keyboards is the size of their buttons. People with severe cases may encounter numerous typing mistakes when the buttons are too close together and maintain a constant size. This difficulty arises due to their challenges in controlling hand movements.

In this context, we propose a novel approach that enhances accessibility through the development of an adaptive keyboard. By utilizing the hovering feature in modern devices, our solution enables zooming in on buttons, significantly improving typing speed and accuracy. Additionally, we offer mechanical support with a stabilizer to secure the hand or arm, enhancing ease, efficiency, and accuracy of movements, providing individuals with a more precise input experience.

Methods: In this project, we utilized two key methods to address the challenges faced by individuals with disabilities. Firstly, we implemented the technology of stylus hovering, enabling precise communication between the stylus and the device's sensors. This integration within our application allows zooming in on keyboard buttons when the stylus hovers above them. As a result, typing accuracy is greatly improved, enhancing the overall user experience.

Secondly, we designed specialized mechanical support devices for individuals with motor disabilities. These devices enable movement in three axes and incorporate circular motion capabilities, crucial for enhancing daily activities. Our approach involved incorporating restraints and elastic springs into the design, countering involuntary movements, and reducing tremor impact. Moreover, the device is adjustable to specific needs, providing personalized support. These assistive technologies play a vital role in improving the quality of life for individuals with motor impairments.

Results: Through an application and mechanical support, the project offers valuable aid to people with disabilities. Zoom functionality boosts accessibility, while improving writing precision. Furthermore, integrating a mechanical support system stabilizes hand movements, empowering individuals by enhancing control over their actions.

Conclusions: Applications and mechanical support aid disabled individuals in overcoming barriers, enhancing accessibility, precision, and stability for hand movements, thus improving their quality of life, and facilitating communication.

Keywords: Motor disabilities, Assistive technology, Adaptive solutions, Accessibility

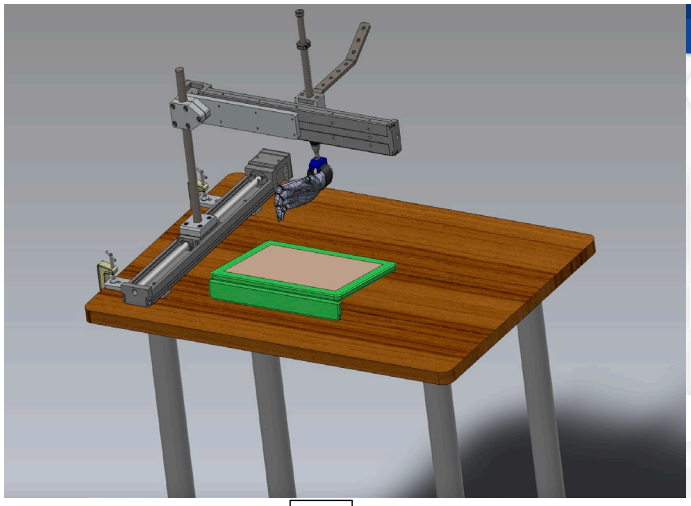

A

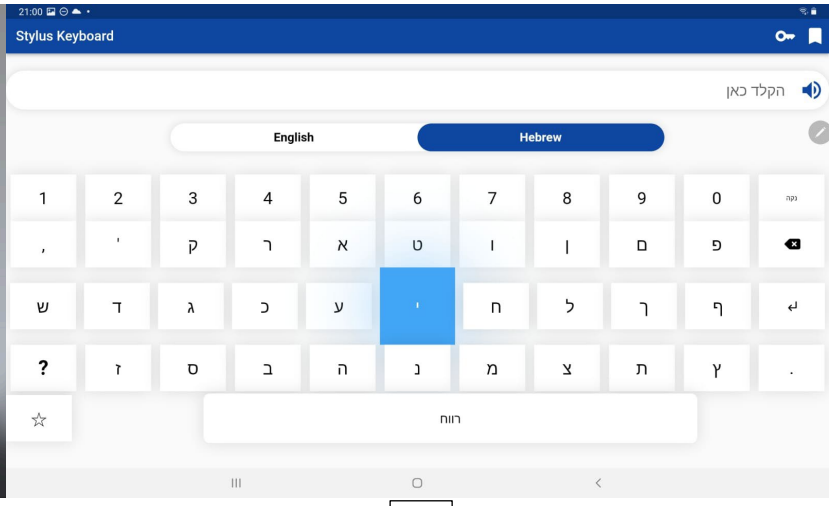

B

Figure A depicts an innovative keyboard that utilizes a hovering feature where buttons enlarge when the tablet's pencil is nearby. Figure B showcases a model that provides mechanical stability for individuals with movements disabilities. It features a specialized brace to support the hand and wrist.

13

Design Of a Platform Used to Measure The Effect Of Antiarrhythmic Drugs On Pluripotent Stem Cell-derived Cardiomyocytes (hiPSC-CMs)

Rotem Solomon[1], Anat Rotschield[1], Savyon Mazgaoker[1], Oryan Karni[2], Merav Belenkovich[3] and Yael Yaniv[1]

[1]Laboratory of Bioelectric and Bioenergetic Systems, Faculty of Biomedical Engineering, Technion-IIT, Haifa, Israel
[2]Laboratory of Stem Cell and Tissue Engineering, Faculty of Biomedical Engineering, Technion-IIT, Haifa, Israel
[3]Laboratory of Cardiovascular Nano-Med Engineering, Faculty of Biomedical Engineering, Technion-IIT, Haifa, Israel

Introduction: Spontaneously beating cardiomyocytes derived from human induced pluripotent stem cells (hiPSC-CMs) have attracted interest due to their ability to generate rhythmic action potentials (APs) similar to the sinoatrial node (SAN) cells. They serve as valuable tools for drug screening and understanding cardiac disease mechanisms. The SAN cell function is controlled by a coupled-clock system whose function has been shown to be mediated by calcium. However, to date, the focus has been primarily on characterizing the electrical activity of hiPSC-CMs to study the effects of drugs on the human heart, ignoring additional factors such as calcium. In this project, we established a protocol for the simultaneous measurement of AP and calcium in single cardiomyocytes and developed an automated analysis program that receives as input the raw data obtained from the microscope and outputs a comprehensive report from which conclusions can be drawn.

Methods: We examined two approaches for the simultaneous measurement of AP and calcium. The first approach was the "CaViar" virus which is a calcium and voltage reporter. The second approach was the combination of two dyes; the membrane potential dye di-8-ANEPPS and the calcium indicator dye Fluo-4 AM.

Results: Cardiomyocytes expressing CaViar exhibited poor AP signal while the combined dyes provided good results. The established dying protocol: experimental dishes were loaded with 2 µM di-8-ANEPPS and incubated at 37ºC in 5% CO_2 for 15 min. The dishes were washed in Tyrode`s solution for 15 min and loaded with 2.5 µM Fluo-4 AM for 20 min in the dark at room temperature. Cells were washed in Tyrode`s solution and imaged with an LSM880 confocal microscope. Di-8-ANEPPS and Fluo-4 AM were excited simultaneously by the 488, di-8-ANEPPS emission was measured at wavelengths of 600-754 nm and Fluo-4 AM was measured at 449-526 nm.

To complete our platform, we designed a GUI Matlab that analyzes the microscope raw data file containing two line-scan images in a few seconds. The GUI detects AP and calcium

transients, as well as LCRs, and calculates beat interval, time to peak, 50% and 90% relaxation time, and LCRs parameters. Furthermore, LCR and AP statistics from the analysis report can be used to classify hiPSC-CMs into 3 types (atrial/ventricular/nodal-like), as previously demonstrated, allowing us to assess a drug effect on specific cell types.

Conclusions: Our innovative platform offers a fast, cost-effective, and reliable method for evaluating the effects of drugs on different hiPSC-CMs types, based on characterization of both AP and calcium signaling.

Keywords: hiPSC-CMs, global calcium release, LCR, action potential.

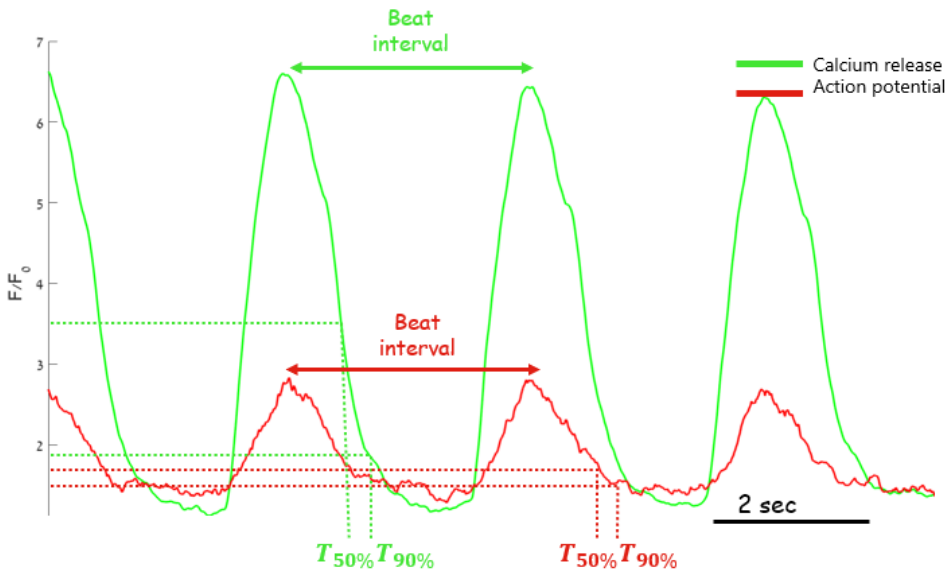

Figure 1: Simultaneous profile of calcium signaling and AP

14

Use of Speech Analysis for the Assessment of Depression and Cognitive Impairment in Elderly People

Shir Singer[1], Maya Goldshalger[1], Daniel Harlev[2] ,Eyal Bergmann[2]

[1] Faculty of Biomedical Engineering, Technion - IIT, Haifa, Israel.
[2] Psychiatric Division, Department of Psychiatry, Rambam Medical Center, Haifa, Israel.

Introduction: Dementia and major depressive disorder (MDD) are debilitating conditions with a significant impact on patients' lives. Currently, diagnosing these conditions relies on subjective face to face clinical assessments. However, there is growing interest in utilizing biological signals, such as acoustic audio features, as a potential diagnostic tool and develop algorithms that can accurately diagnose MDD and cognitive decline. Voice-based tests can be easily conducted over the phone or through telemedicine, making them accessible and practical. The development of such an algorithm would provide an objective and automatic method for diagnosing MDD and dementia, enabling early diagnosis and intervention. This advancement could significantly improve the diagnosis and management of these conditions, leading to better outcomes for patients.

Here, we present a comprehensive approach, showcasing the full cycle from data gathering to feature engineering, statistical analysis, and prediction models, aimed at developing accurate algorithms for diagnosing MDD and cognitive decline.

Methods: Recordings were obtained from 33 patients at the Psychogeriatric clinic, with three recordings per patient. The signals underwent preprocessing to enhance quality and reduce noise. Through feature engineering using windowing technique. The potential correlation of these features with MDD and cognitive decline was assessed using AUROC (Area Under the Receiver Operating Characteristic curve). Cross-validation was employed during feature selection process to ensure robustness, and the features were selected based on the median AUROC scores. Machine learning algorithms, including Logistic regression, SVM, and Random Forest, were subsequently utilized to develop prediction models using the selected features. Model training and evaluation involved rigorous cross-validation methods to assess reliability and generalizability.

Results: Modeling based on the selected features yielded notable results. For cognitive impairment, Random Forest and Logistic Regression models achieved an accuracy of 80% on a test set of size 10. Similarly, in the case of MDD, a single Random Forest model achieved an accuracy of 70% on test set of size 10.

Conclusions: Our study highlights the potential of voice-based acoustic audio features as a diagnostic tool for MDD and cognitive decline. By employing feature engineering and machine learning algorithms, the preliminary results show promising accuracy rates in diagnosing cognitive impairment and depression. This research paves the way for improved early detection and intervention strategies, leading to better outcomes for patients.

Keywords: Cognitive decline, Major Depressive Disorder (MDD), audio signal processing, machine learning algorithms

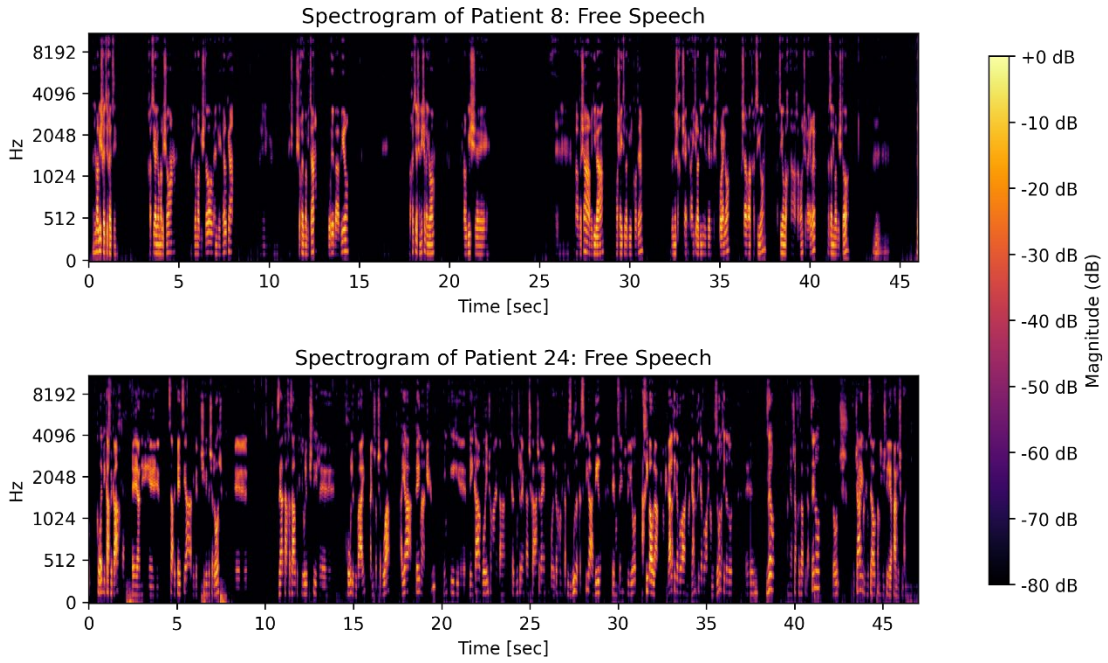

Figure 1: Two spectrograms comparing the free speech records of two patients. Patient 8, who tested positive according to the GDS (Geriatric Depression Scale), is shown in the top spectrogram, while patient 24, who tested negative, is shown in the bottom spectrogram. The differences between the two patients can be observed through the variations in darker regions and frequency patterns within the spectrograms.

15

Deep-learning-based Registration for Hippocampal Atrophy Detection in aging and Alzheimer's disease

Habib Azzam[1], Yazan Nasser[1], Samah Khawaled [2], Gaia Levin[1], Moti Freiman[1]

[1] Faculty of Biomedical Engineering, Technion - IIT, Haifa, Israel
[2] Faculty of Applied Mathematics, Technion - IIT, Haifa, Israel

Introduction: Alzheimer's Disease (AD) is a prevalent and irreversible neurodegenerative disease and the leading cause of dementia worldwide. A new AD diagnosis occurs every 3 seconds, affecting 55 million people in 2020. By 2050, this number is expected to reach 139 million.

Structural MRI imaging is one of the leading diagnostic tools for AD, as it can be used to detect hippocampal atrophy, a common symptom of AD and mild cognitive impairment (MCI). Detecting this requires image registration, used to morph a selected image to the same reference frame as a reference image and facilitate comparison between the images. However, current detection methods using this technique are time-consuming and prone to inaccuracies.

To address this, we utilized the deep learning (DL) registration model, Voxelmorph, developed by A. Dalca et al. Such DL systems enable a faster and more accurate image registration tool for AD diagnosis. Our pipeline aims to provide an automatic, efficient, and accurate image registration network.

Methods: We trained our model using data from the Alzheimer's Disease Neuroimaging Initiative (ADNI) database. The dataset includes 3D T1 weighted MRI images - 18 AD, 37 MCI, and 34 control (CN) patients along three visits. The image dimensions are $160 \times 192 \times 224$. The images were preprocessed using intensity normalization and affine registration was performed. Segmentation masks of left and right hippocampus were extracted using a pre-trained neural network called hippodeep.

We evaluated the results by applying the trained network's deformation field to segmented left and right hippocampus masks then calculating the percentage volume change (PVC) between visits. We compared our method with the classical deformable registration method ANT's, by calculating PVC change between the second and third visits relative to the first visit.

Results: Significant differences in mean PVC were observed. For example: the mean PVC for AD patients was – left hippocampus -42.67 for the first pair, and -46.17 for the second pair, and for the right hippocampus -4.52 for the first pair, and -16.78 for the second pair.

Figure 1 highlights greater PVC change in AD patients compared to MCI patients. In addition, Figure 1 indicates that the DL method exhibits more negative PVC change between visits compared to the ANT's method.

Conclusions: Our results indicate that deep learning registration methods can successfully be used for detecting hippocampal volume loss in AD and MCI patients, while outperforming the classical method ANT's both in accuracy and in run time.

Keywords: Deep Learning, Image Registration, MRI, Alzheimer's Disease

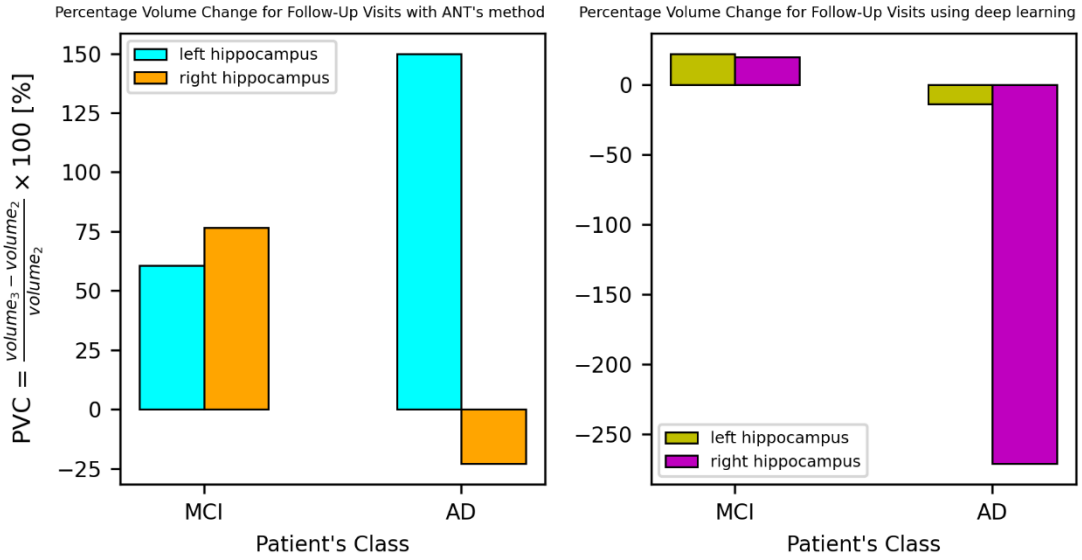

Figure 1: A comparison of the PVC between second and third visits calculated for the ANT's classical image registration method (left) and DL method (right) for deformable registration.

16

Differentiating reading gains in children with attention deficit hyperactivity disorder and children with reading difficulties objectively using fMRI data and machine learning

Masa Khashab, Sanad Ghanaiem, Tzipi Horowitz-Kraus, Rula Farah

[1] Faculty of Biomedical Engineering, Technion - IIT, Haifa, Israel
[2] Faculty of Education in Science and Technology - IIT, Haifa, Israel

Introduction:

Reading is the ability to decode printed text and comprehend it's meaning, the process of reading relies on different sub-processes and executive functions (EF) which determine the performance of reading process. Researchers suggest that EF are associated with different neural networks and affected by their activity.

Dyslexia or Reading Difficulties (RD) is a neurodevelopmental disorder that affects reading ability among 7% of children in primary school according to researchers. Researchers also show that RD has a high rate of comorbidity with attention deficit hyperactivity disorder (ADHD). A different neurodevelopmental disorder characterized by inattention, impulsiveness, and hyperactivity.

In our research we will explore the effect of EF-based intervention on both executive functions' performance and functional connectivity of neural networks and the correlation of gain between them in different groups of participants. test the ability of implementing machine learning principles by using fMRI acquisition prior to intervention to predict gain.

Methods: behavioral and neural data were collected from three groups of children. 17 typical readers (TR), 17 children with RD- only and 19 children with both RD and ADHD. In the first stage, all participants went through behavioral assessment tests. In addition, fMRI acquisitions record neural activity. In the second stage children participated in training by using EF-based program. A program with unique training style of training. The participants are required to read different sentences while the letters are deleted from the left to the right side in a specific pace. Subsequently, the Participant should answer a question regarding the sentence he read. Deletion pace is updated according to the participant performance. In the final stage, behavioral assessment tests and fMRI acquisitions are conducted again to measure the effects of the intervention.

In order to analyze the fMRI data and find the correlation with the behavioral results we used conn program. By using conn the change in functional connectivity was measured for each participant before and after intervention per each region of interest (ROI) and correlated with gain for each skill measured during the assessment tests.

Results: Statistical results show that training had a different effect among the three groups. Level of gain varied among the different skills measured. The change in functional connectivity per region was also different between the groups. In addition to that, gain in several skills was highly correlated with functional connectivity level in (or between) several neural networks before training.

Conclusions: the high correlation detected between functional connectivity within or between specific neural networks among the different groups provides indications about the effect of EF-based training. Besides that, high correlation between function connectivity prior to intervention and gain in specific skills indicate that gain level can be predicted prior to training based on fMRI acquisitions by implementing machine learning principles by providing a larger sample size and higher resolution analysis regarding fMRI acquisition.

Keywords: Executive functions, functional connectivity, behavioral, Gain.

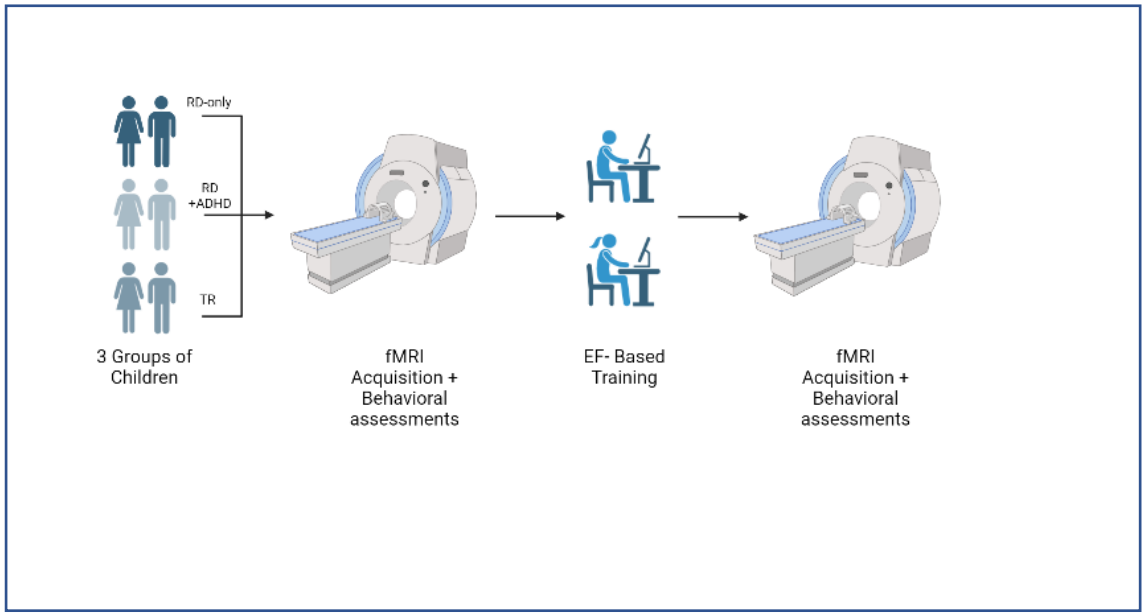

Figure 1: Study Procedure

17

Chronic obstructive pulmonary disease diagnosis from oximetry time series

Shir Hadad[1], Hadar Cohen[1], Jeremy Levy[1]

[1] Faculty of Biomedical Engineering, Technion - IIT, Haifa, Israel

Introduction: Chronic Obstructive Pulmonary Disease (COPD) affects more than 300 million people worldwide, making it a prevalent respiratory condition and a leading cause of death among respiratory diseases. Early diagnosis is crucial for effective symptom management, slowing disease progression, and improving the quality of life for patients. However, the current gold standard diagnostic method, spirometry, faces challenges in terms of accessibility and the need for specialized training. Furthermore, spirometry may have limitations in detecting COPD in its early stages, as lung function impairment may not be significant enough to produce abnormal results. In our project, we propose harnessing the benefits of pulse oximetry—a cost-effective and patient-friendly test that can be performed comfortably from home. By integrating pulse oximetry with machine learning techniques, we aim to develop a predictive model for early COPD detection, overcoming the limitations of spirometry and enabling timely interventions to optimize disease management outcomes.

Methods: In our study, we utilized a database of oximetry readings from 370 patients from Spain and France, including COPD status information. We analyzed the signal using a windowing approach in which each signal was divided to 3-hour windows to capture temporal patterns and reduce noise. Three machine learning models - Random Forest, Support Vector Machine (SVM), and Logistic Regression, were trained and evaluated on these windows. To ensure robust evaluation, the decision was taken according to the "majority vote" across these windows.

To capture relevant information from the oximetry data, we employed feature extraction techniques, including the analysis of SpO_2 trends, respiratory patterns, and measures related to desaturation events and pulse rate variability. Additionally, to optimize the models' performance, we utilized feature selection methods such as K best and Lasso regularization. Due to class imbalance challenges, we implemented data augmentation techniques. This included the application of the Synthetic Minority Over-sampling Technique (SMOTE). By augmenting the minority class and mitigating the impact of class imbalance, these techniques improved the accuracy and robustness of the models.

Results: Through extensive error analysis, we gained valuable insights into the Random Forest model, which stood out as our most successful model during the development process. Nevertheless, we recognized the importance of considering the results of the other two models to strengthen the final decision. For instance, to classify a patient as "Healthy," at least two out of the three models must classify him as such.

Conclusions: Oximetry-based approach, coupled with machine learning, showed promise for early diagnosis. Key features include decreased oxygen saturation (SpO_2) levels, fluctuations, and desaturation events. Further research can unlock its full potential in improving patient outcomes and enabling effective disease management.

Keywords: COPD, Machine Learning, Oximetry.

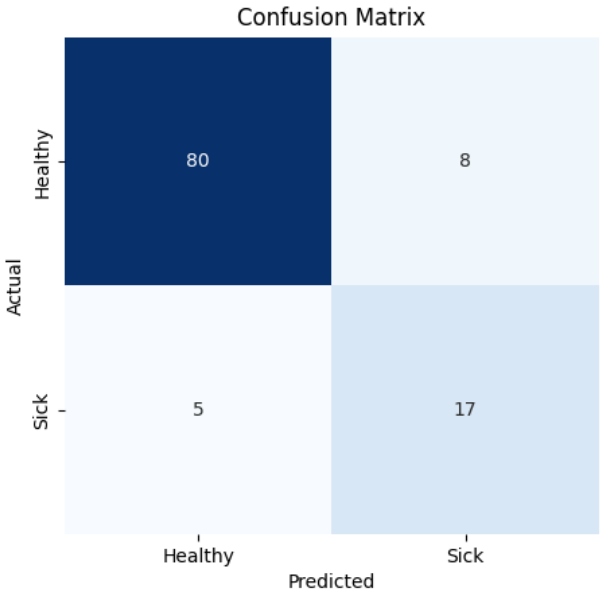

Figure 1: confusion matrix

18

DNA Origami Structure for Improving Gene Editing by CRISPR/Cas9

Dana Gal[1], Ronnie Itzhaki[1], Hadas Omer[1], Gaia Levin[1], and Yuval Garini[1]

[1] Faculty of Biomedical Engineering, Technion - IIT, Haifa, Israel

Introduction: CRISPR/Cas9 technology is a gene editing method that uses an RNA sequence and a Cas9 protein to cut the DNA in a specific target site. A drawback of this system is its lack of specificity. For Cas9 to carry out the cut, the guide RNA must bind to a site in the DNA. There is a high probability of the RNA binding to DNA sequences that are similar to the target sequence (off-target sites), leading to unintended cutting and genetic damage. In this study we propose a design for a nanometric DNA origami structure that would create a complex with CRISPR/Cas9, to reduce off-target effects and increase binding specificity.

Methods: DNA origami is a technique in nanotechnology where DNA molecules are folded into specific shapes and structures. The method of creating DNA origami involves utilizing single-stranded DNA molecules as a scaffold for the structure, and incorporating shorter complementary DNA strands called staples to form precise interactions. This interaction between the scaffold and staples results in the formation of a specific, predetermined three-dimensional shape.

Results: We designed a DNA origami nanometric structure. This 100-nanometer rod-shaped structure has a flexible section in the middle and two binding sites, one on each side. One end of the rod is connected to the RNA component of the CRISPR/Cas9 complex, while the other end features a single-stranded tail that serves as an additional target sequence to a specific DNA location 100 nanometers away from the CRISPR/Cas9 target site. In addition, the design of our DNA origami - CRISPR/Cas9 system consists of a block sequence which hinders the target site in the RNA, which will disconnect once the complex is in prolonged proximity to the DNA target site. For designing the structure, we used a special software called CaDNAno. To decide on the sequence that would serve as the additional sequence we conducted a statistical evaluation regarding the folding of the DNA in the cell, followed by BLAST tool to find the required sequence.

Conclusions: We have designed an original DNA origami structure designated for increasing the specificity of the CRISPR/Cas9 gene editing complex. This complex requires the binding of two specific sequences with a defined distance between them, while blocking the RNA binding site. The basis of this approach is that adding a second target sequence may increase the binding specificity to the target region, as the probability of finding two such specific sequences is much lower than that of finding one sequence only. Future investigations should involve the validation of the capacity of the CRISPR/Cas9-DNA origami complex to successfully enter a viable cell and its nucleus. Furthermore, it is essential to explore the

consequences of integrating the DNA origami structure on the specificity of CRISPR/Cas9 DNA cutting sites.

Keywords: CRISPR/Cas9, DNA Origami, off-target

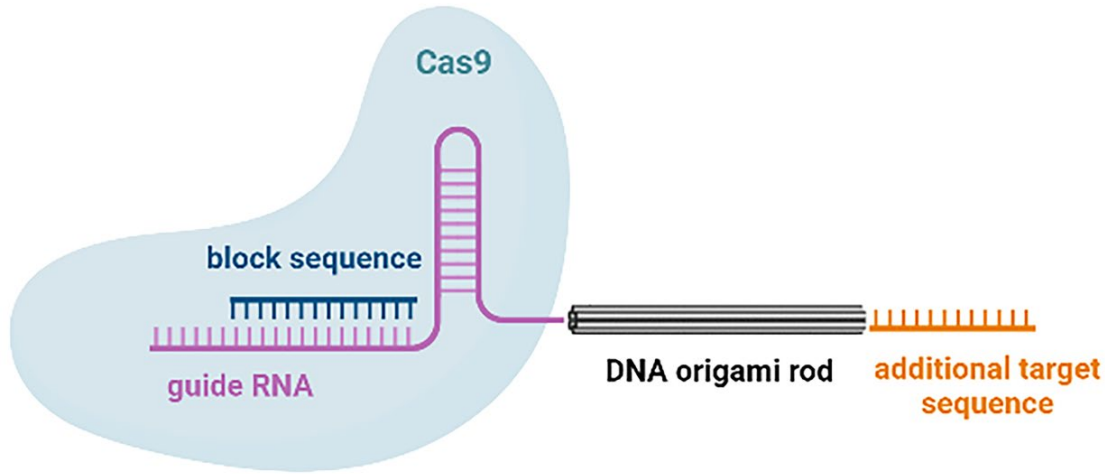

Figure 1: an illustration of the DNA origami – CRISPR/Cas9 system

19

Electrostatic Effects on Inhaled Aerosol Deposition in the Lung Bronchi

Morane Elbaze[1], Leo Ibghi[1], Ron Bessler[1], and Josué Sznitman[1]

[1] Faculty of Biomedical Engineering, Technion - IIT, Haifa, Israel

Introduction: Aerosols generated by off-the-shelf inhalers are known to acquire significant quantities of net electrical charge before entering the respiratory tract. Particle deposition in the lungs relies on several fundamental mechanisms such as viscous drag, gravitational sedimentation, electrostatics, and diffusion. Since the electrostatic force is inversely correlated with the square of the distance between an aerosol and the airway wall, it has long been acknowledged as having significant potential to enhance deposition in the deep lung. However, because of the difficulty to study such phenomena directly, *in vitro* research has mostly focused on models limited to the upper airways.

Here, we present a microfluidic channel mimicking the anatomy of the respiratory tree's 11^{th}, 12^{th}, and 13^{th} deep generations, to evaluate the importance of electrostatic effects on micron and submicron-inhaled aerosol in the deep lung.

Methods: We designed and fabricated *in vitro* models of the lung respiratory tree, using 3D-printed molds filled with polydimethylsiloxane (PDMS). To recreate electrical conditions similar to those present in the lungs, we cover our region of interest with a thin layer (30nm) of indium tin oxide (ITO). Since ITO is transparent as well, we did not compromise the glass transparency, enabling us to obtain the particle deposition pattern.

We worked with fluorescent polystyrene latex (PSL) particles in two distinct monodisperse aerosol sizes, micron: dp = 1.1µm and submicron: dp = 0.5µm, produced by aerosol generator (Model 3076, TSI) with ambient air as the gas source. To mimic quiet breathing flow conditions, we used a syringe pump (PHD Ultra) connected to the channels' outlet. We electrically grounded the coated glass to guarantee an identical electrical setup before each deposition assay. Since the atomized PSL particles are intrinsically highly charged during the aerosolization process, as a control group we compare the same aerosolized particle sizes under neutralized conditions using an electrical ionizer (1090 MSP, TSI). Particle deposition in the models was captured using a fluorescence inverted microscope and the pictures were processed using ImageJ and MATLAB.

Results: Electrostatic effects have a significant influence on particle deposition in the respiratory tract, different sizes behave differently to the electrostatic. For the 1.1µm large particles governed by gravity, the electrical charge increases the probability of deposit. For 0.5µm submicron charged particles, we observed a significant increase in deposition and additionally a new distribution pattern compared to the neutralized case. We strengthen our

observations via numerical simulations of the nonlinear electrostatic force equation and non-dimensional analysis.

Conclusions: Electrostatic alters the deposition pattern not only in the upper airway but also in the small bronchioles. Hence, electrostatic consideration should take place rather than be completely discarded, especially for the submicron. For medical use, this knowledge on electrostatics can potentially enhance the low efficiency of inhalers for drug delivery.

Keywords: Microfluidic, Drug Delivery, Electrostatic Effects, Aerosols Deposition.

Figure 1: Deposition Pattern in the deep lung model for 2 cases of study.

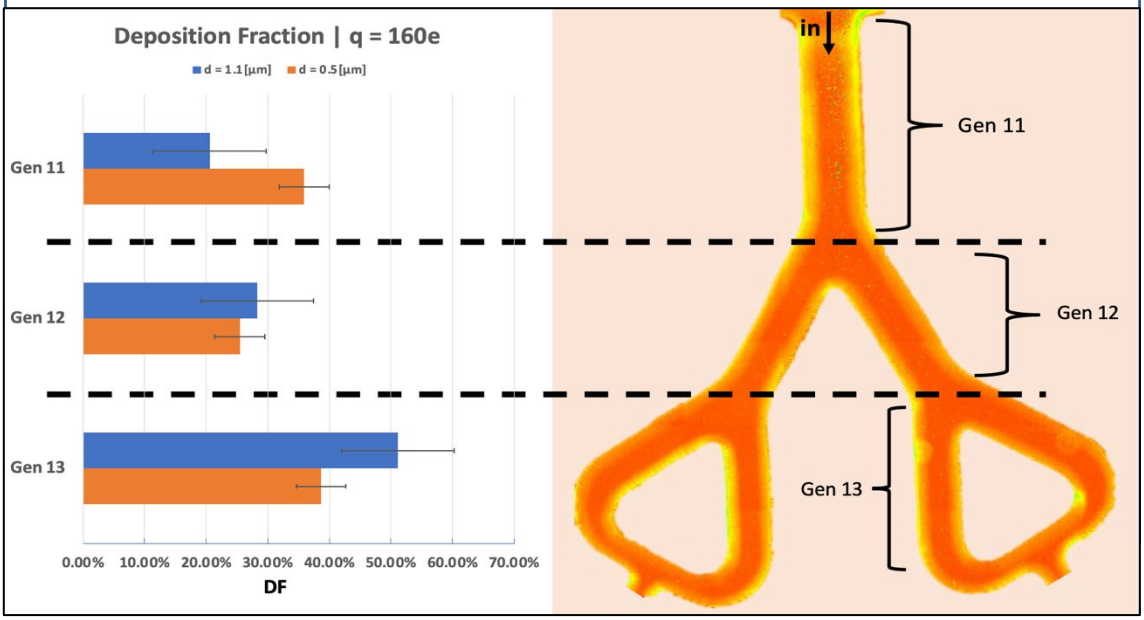

20

Predicting Clinical Response to Radiotherapy Treatment in CRC Patients

Bashar Khoury[1], Jeries Saleh[1], Yinon Goldstein[2], Noam Keidar[1], Yonatan Elul[2] and Assaf Schuster[2]

[1] Faculty of Biomedical Engineering, Technion - IIT, Haifa, Israel
[2] Faculty of Computer Science, Technion - IIT, Haifa, Israel

Introduction:

Colorectal Cancer, a fatal subtype of colon cancer, is common among cancers in western countries. The biological and morphological characteristics of the cancer make it clinically challenging, therefore, radiotherapy is mostly used to treat it. However, only in ~28% of the cases will the treatment lead to a complete clinical response. Therefore, computer-aided diagnosis can be used to increase accuracy in predicting the effectiveness of radiotherapy. We propose to train a deep learning model which can predict either 'no clinical response', 'partial clinical response' or 'complete clinical response' for tumor, metastasis, and lymph nodes, along with post-therapy tumor stage, given annotated computed-tomography scans along with clinical data from Rambam Hospital.

Methods:

First, we preprocessed the clinical data on which we fit a MultiOutputClassifier with Random Forest as a baseline. Since our data is limited in quantity, the results were decent. However, since we are dealing with medical data, accuracy and reliability are on the top of our priorities. Therefore, we employed a convolutional neural network model based on ResNet50 to consider the computed-tomography scans. ResNet's unique architecture allows training deep neural networks which achieve state-of-the-art results in computer vision tasks. We modified ResNet50 to effectively process volumetric data derived from CT scans, enabling analysis and interpretation of the three-dimensional anatomical structures.

Results:

Using a MultiOutputClassifier with Random Forest, we managed to get a prediction accuracy of 80.61% on the test set. While demonstrating a satisfactory level of performance, the mentioned model doesn't meet the required accuracy standards for medical applications. Several experiments are currently under way using the modified 3D ResNet50 model, alongside models of greater complexity such as token-to-token vision transformers, that potentially exhibit enhanced capabilities in mitigating the limitations arising from insufficient data.

Conclusions: Computer-aided diagnosis can be used to give fairly accurate indications about the output of the radiotherapy treatment before it is done. We hypothesize that using state-of-the-art computer vision algorithms coupled with the integration of domain knowledge achieve higher accuracy and reliability. By leveraging the advancements of the deep learning field alongside the expertise of medical professionals, doctors may acquire valuable insights and assistance in treatment planning, which ultimately improve treatment outcomes in radiotherapy.

Keywords: Deep Learning in Healthcare, Colorectal Cancer, 3D Computer Vision, Radiotherapy Outcome Prediction.

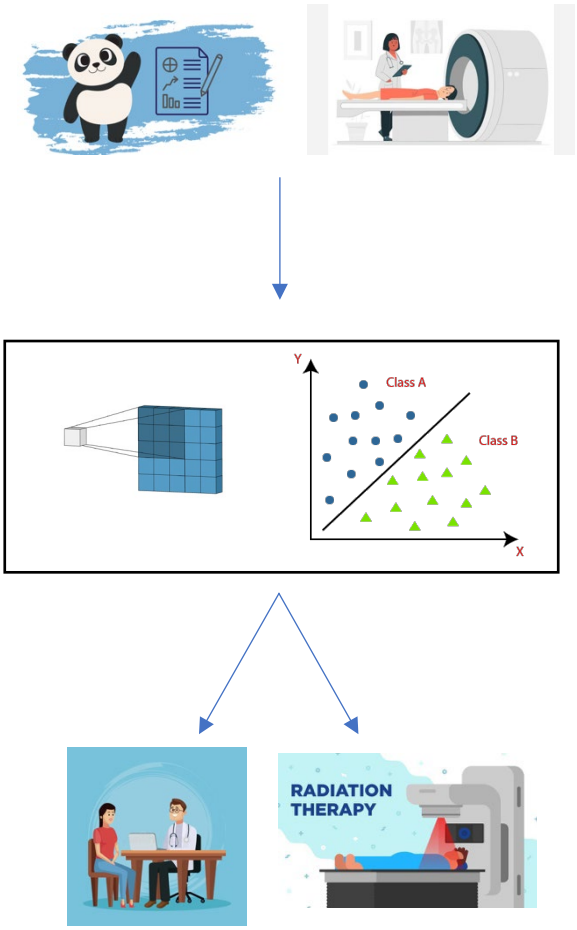

Figure 1: An overview of the framework: The doctors gather clinical data and CT scans, which is preprocessed and put into the model, and consider its prediction to decide a suitable treatment.

21

Phantom-Based Characterization of Human Skin Tissue and Blood Vessels for Preliminary In-Vitro Blood Count Experiments

Oshri Hemo Ferraro[1], Tal Darbinovski[1], Reut Friedman[2], and Dvir Yelin[2]

[1] Faculty of Biomedical Engineering, Technion - IIT, Haifa, Israel
[2] Faculty of Biomedical Engineering, Biomedical Optics Lab, Technion - IIT, Haifa, Israel

Introduction: Blood cell counting is a vital diagnostic tool used for monitoring treatment response, diagnosing medical conditions, and assessing disease severity. However, current methods involve invasive blood extraction, posing drawbacks such as patient discomfort, infection risk, and limited accessibility in newborns. To address these challenges, a non-invasive approach based on optical microscopy of blood cells in vivo has been proposed. This innovative method, utilizing flow cytometry, enables visualization of cell morphology and dynamics in the blood circulation, providing essential information for blood cell counting. To implement this technique in living organisms, it is crucial to investigate the light absorption and scattering properties in tissues and develop accurate phantoms to simulate tissue activity, thereby enhancing the method's efficiency and applicability.
Our project focuses on developing and characterizing a phantom that mimics human skin tissue and blood vessels. This phantom will provide insights into light absorption and scattering in tissue, facilitating the application of in vitro blood cell counting.

Methods: The creation and characterization of the PDMS phantoms involved several steps. Initially, a mixture of PDMS and cross-linking material was poured into a mold, with the addition of glass particles for enhanced properties. After thorough mixing, the molds were placed in a desiccator to achieve a smooth surface, and then spin-coated to achieve the desired thickness. Subsequently, the molds were cured in an oven. Simultaneously, an optical array was constructed, comprising mirrors, a laser, and an integration sphere, ensuring stable sample positioning for precise measurements. The optical properties of the phantoms were determined using the inverse adding doubling(IAD), which involved measuring light transmission, reflection, and noise levels. The collected spectral data were analyzed to estimate the total absorption and scattering coefficients. This analysis aimed to establish the relationship between these coefficients, the phantom thickness, and the pores:PDMS ratio.

Results: To draw conclusions, we conducted a series of measurements to determine the absorption and scattering coefficients of the tested phantoms. Our findings revealed a clear trend: for phantoms with constant pores: PDMS ratio (1:4), increasing the thickness resulted in higher values for both absorption and scattering coefficients. Additionally, we examined phantoms with uniform thickness (0.02 and 0.03 mm) but varying pores:PDMS ratios. In this case, we observed that higher ratios corresponded to greater absorption and scattering coefficients.

Conclusions: Based on our results, it is evident that increasing the thickness of the phantom and the concentration of pores: PDMS leads to a significant increase in the obtained absorption and scattering coefficients. This observation is logical since the presence of pores in the PDMS material facilitates light absorption and scattering, as PDMS itself lacks inherent optical properties.

Keywords: spin-coating, optical array, integration sphere, inverse adding doubling (IAD)

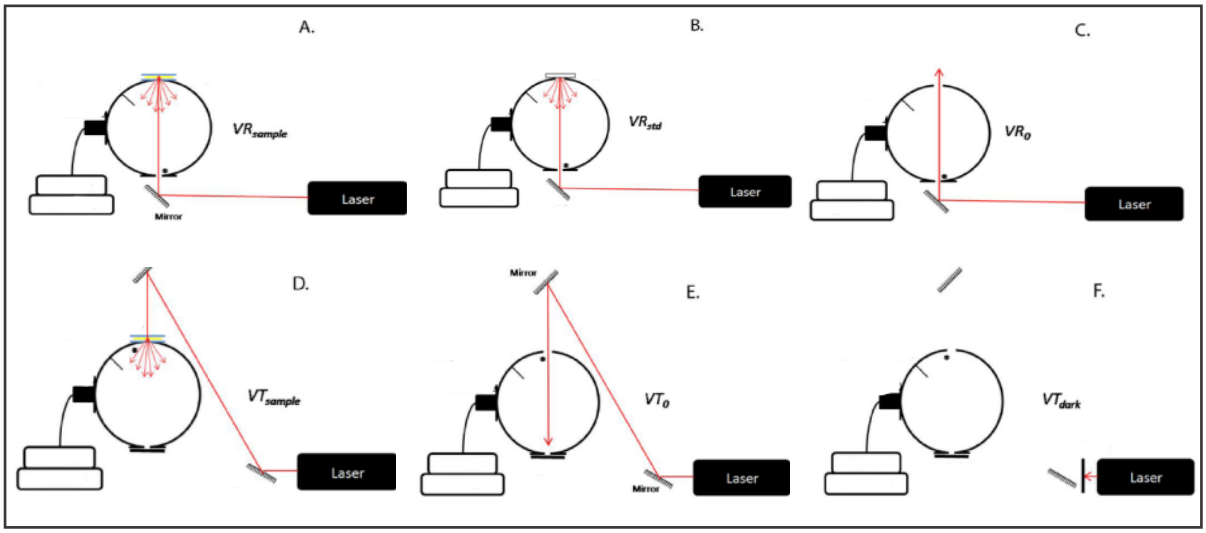

Figure 1: Schematic representation of the experimental setup: A-C for reflection measurements, D-F for transmission measurements.

22

Cancer cells as a drug delivery system for Osteosarcoma

Maya Naim[1], Roy Meretzki[1], Orr Bar Natan[1,2], and Yosi Shamay[1]

[1] Faculty of Biomedical Engineering, Technion - IIT, Haifa, Israel
[2] Nanomedicine and Nanotechnology Interdisciplinary Program, Technion - IIT, Haifa, Israel

Introduction: Osteosarcoma (OS) is the most common type of bone cancer in children and young adults- Approximately 1,000 new cases of osteosarcoma are diagnosed each year in the United States. The standard treatment for OS is a combination of surgery and chemotherapy, which has significant long-term side effects, depending on the severity of the cancer, and it has not changed in the last 30 years. Metastatic OS has a 30-40% recurrence rate and a > 70% mortality rate.

Here we offer a novel drug delivery system based on lysosomal trapping, a process in which drugs accumulate into lysosomes and other cellular acidic compartments. Our objective is to leverage this mechanism for entrapping drugs within cancer cells, effectively transforming them into carriers capable of delivering therapeutic agents directly to the intended target cells.

Methods: In our study, we employed the K7M2 murine cell line as a dual-purpose system, serving as both carrier cells and target cells, to evaluate the effects of various treatments. We cultured the K7M2 cells and subsequently seeded them into a 96-well plate.

To generate drug-loaded cells, we subjected the same K7M2 cell line to incubation with different Kinase-inhibitor drugs of interest, both as free drugs and in the form of nanoparticles (NPs): Ponatinib, Nintedanib and Trametinib. Following incubation, a serial dilution of the drug-loaded cells was used.

To comprehensively assess the effectiveness of the treatments, we implemented a multifaceted approach. Firstly, we used automated microscopy to capture high-resolution images of the cells within the wells. We utilized drugs with inherent fluorescent properties to precisely monitor the process of drug penetration into the target cells. Additionally, to obtain quantitative data on cell viability, we employed the CellTiter-Glo® (CTG) assay. This assay utilizes luminescent signals generated through ATP detection to measure cell viability accurately.

Results: In free drug experiments, a different dose response was observed for each drug. In the experiments involving drugs and NPs entrapped in carrier cells, significant cell death was observed. Notably, we also observed dose responses among the different drugs in this experimental framework. Importantly, these findings were consistent across both our two-dimensional (2D) and three-dimensional (3D) experimental setups.

Conclusions: The loaded cells successfully released the drugs, that defused into the target cells and produced cells' death. These results show the potential of lysosome trapping as a drug delivery system. We believe that this method has a potential to reduce drugs toxicities to normal

tissues by better targeting, and future research should focus on optimizing the process and test this hypothesis *in vivo*.

Keywords: Osteosarcoma, lysosomal trapping, drug delivery system,

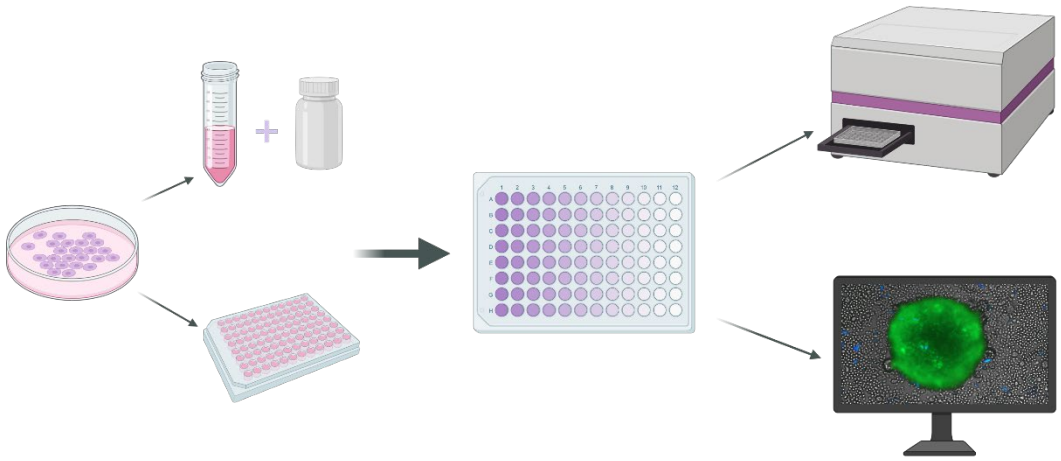

Figure 1: Workflow of an experiment, which includes creating drug-loaded cells and assessing the impact of serial dilution of carrier cells on target cells, using microscopy and a CTG viability test.

23

Video-Based Lie Detection: Unveiling Truth through Heart Rate Variability

Shir Eitan[1], Inbar bar[1], Ido Weiser-Bitoun[1], Moran Davoodi[1], and Yael Yaniv[1]

[1]Faculty of Biomedical Engineering, Technion - IIT, Haifa, Israel

Introduction:

Nowadays polygraph, a device targeted to determine whether a subject is lying according to biological data, has many flaws that harm its reliability and its reputation. Most of the polygraph's disadvantages are due to dependency on the polygraph examiner and the multitude of measuring systems involved in the process. Here we demonstrate the feasibility of a new lie detection method that is based on an algorithm for detecting heartbeats from a video film of a subject's face, while using an advanced Heart Rate Variability (HRV) analyzing tools. The use of measured heartbeats relies on previous findings according to which the HRV changes in stress conditions. This innovative method can be a substitute or an addition to the existing polygraph method and can provide a solution to some of its shortcomings. For example, it provides partial automation thus limiting the effect of the examiner's expertise on the results. Additionally, its detection tool (a video camera) is wireless, thus reducing noises resulting from subject's movements. A significant innovation brought by this tool is the ability to perform credibility check for any person ever recorded by video camera for any reason.

Methods:

We started with collecting, rewriting and testing relevant Matlab codes for future signal processing and analysis. Later, we have conducted clinical trial that included heartbeat recording at rest for fifteen minutes using three different measuring methods simultaneously – Electrocardiogram (ECG), Photoplethysmogram (PPG) and a video camera, and an additional similar recording where the subjects were asked to answer six true or false questions. Then, Using Matlab, we calculated the heartbeats intervals as measured by each of the methods. For each participant's set of signals, noisy segments were excluded and relatively clean signal segments of at least ten minutes were kept for analysis. For the questions part analysis, we have looked for changes in HRV measures when the subject answered truth or a lie. The changes in HRV were examined by a statistical test. The RR intervals were calculated and processed with the "PhysioZoo" platform that offers physiological time series analysis.

Results:

When comparing the RR intervals' histogram of the truth and lie sections of the records (in all measuring methods), there is a high similarity in values, as seen in figure 1.

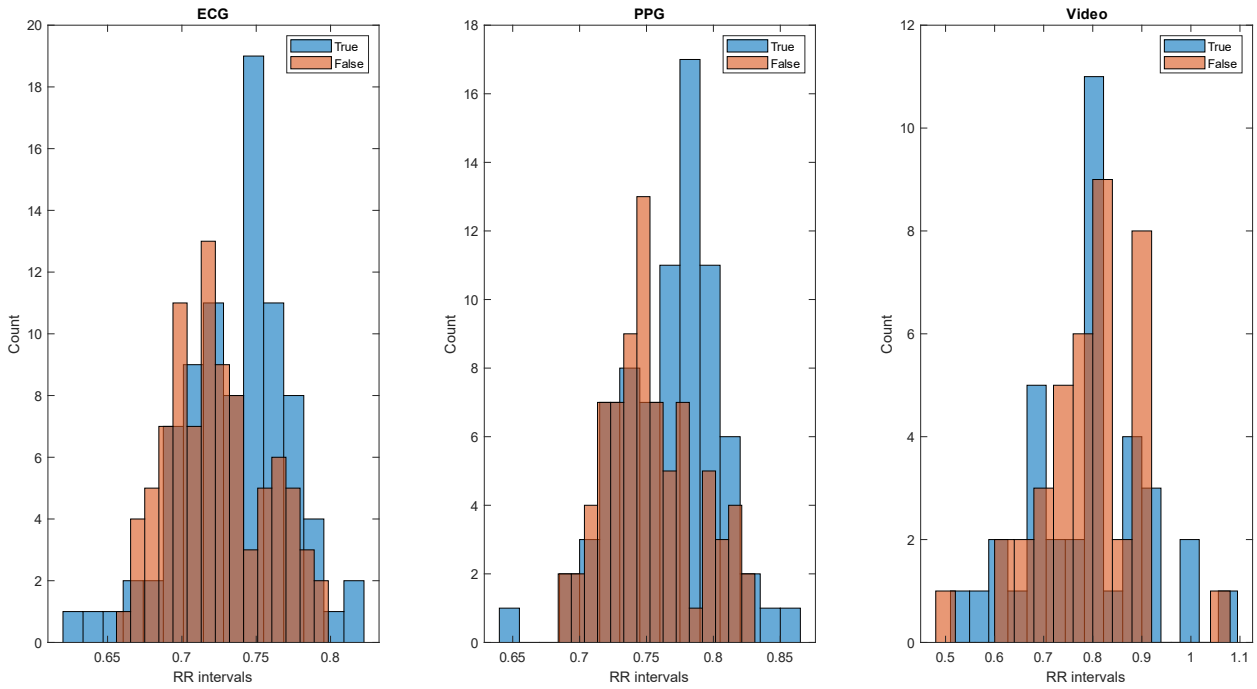

Figure 1 – Histograms of RR intervals in a single subject's truth and lies sections, as measured by three different methods

We used Wilcoxon statistical test to determine whether the RR intervals in the truth sections are different than those of the lie sections. For 5 out of 9 subjects, we found significant difference (p-value < 0.05) between the lie and truth sections, thus presenting a proof-of-concept to our novel method.

Conclusions:

We presented here a novel method for video-based lie detection, which can be used as a wireless polygraph. Such method can be used in a variety of fields and situations. Further work is needed to maximize the potential of our unique method, such as increasing the subject number and improving the lie-detection algorithm.

Keywords: Polygraph, Electrocardiogram, Photoplethysmogram, RR intervals, Signal Processing.

24

Diffusion Model Simulator

Maia Lehrman[1], Tav Nahimov[1], Alon Saguy[1], Gaia Levin[1], Yoav Shechtman[1]

[1]Faculty of Biomedical Engineering, Technion - IIT, Haifa, Israel

Introduction: Deep learning algorithms are effective in addressing various challenges in the field of microscopy, but acquiring large numbers of labeled images for training those algorithms is time-consuming. Current methods use physical models to generate images, but this overlooks important structural features. Our solution is a simulator based on diffusion models that generates high-resolution microscopy images for training networks, eliminating the need for extensive image acquisition. This project's novelty lies in its ability to utilize neural networks for generating a diverse range of biological images, surpassing the capabilities of simpler models.

Methods: To implant our simulator we used a novel neural network architecture known as the Diffusion Model that has recently been introduced. This model is based on iterative denoising and consists of two main components: forward and reverse processing. In the forward process, an image undergoes multiple transformations with the addition of nonlinear noise until it becomes pure noise following a Gaussian distribution. By reversing the process and gradually reducing the amount of Gaussian noise, we can uncover an image. This iterative approach allows us to simulate new images by introducing different Gaussian noise each time, resulting in distinct images. The objective of a neural network is to learn the appropriate weights that gradually eliminate the noise, thereby reconstructing the training set images. Once the model is trained, we can introduce new noise and generate new data.

Results: We were able to use the diffusion model to generate visually appealing microtubules and mitochondria images. The next step would be to determinate scientific quality and their superiority over existing data. We will evaluate our simulated data on a known model called CARE (Content-Aware Image Restoration). The evaluation will enable us to ascertain the suitability of our generated images for use by researchers. In addition, we successfully created a GUI (Graphical user interface) using "tkinter" in python in order to enhance the user experience of the simulator, making it more comfortable and easier to use.

Conclusions: We developed a unique image simulator that can generate high resolution microscopy images of several biology organelles. This will allow researchers to generated fast a large amount of high-resolution microscopy image that are more realistic than today current methods. Future work on this project can be to expand the organelles this model can generate, and to use different image sizes, different SNR (single noise ratio), thus larging the potential

of this project to be adapted by grater many researches that need to train their neural networks on a large amount of data.

Keywords: Diffusion model, high resolution microscopy images, image simulator, neural networks

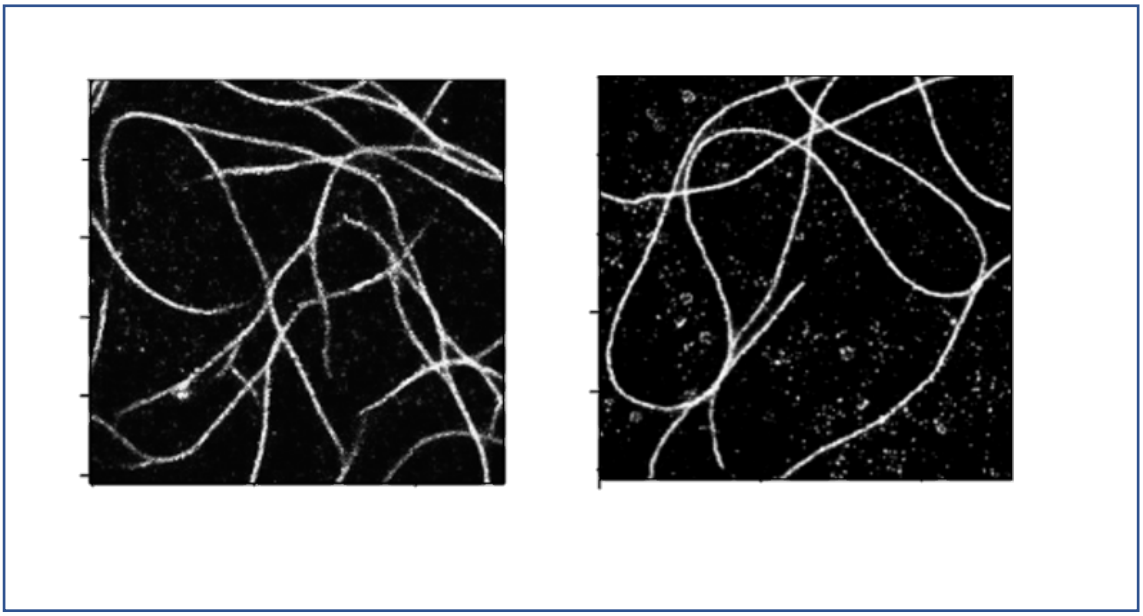

Figure 1: on the left: a "fake" image of microtubules generated by the diffusion model simulator, on the right: a real image of microtubule acquired with a microscope.

25

Quantification of diabetic infarct healing with multimodal imaging using optomagnetic nanoparticles

Noa Levi[1], Maya Sharoni[1], Betsalel Elgrably[1], and Katrien Vandoorne[1]

[1] Faculty of Biomedical Engineering, Technion - IIT, Haifa, Israel

Introduction: Diabetes mellitus type 2, is one of the major emerging health concerns of the 21st century. Diabetics are highly vulnerable to the development and progression of atherosclerosis and related diseases, such as myocardial infarction (MI). MI occurs because a coronary artery occludes, resulting in myocardial cell death and necrosis. Subsequently, an inflammatory response is initiated, wherein inflammatory monocytes/macrophages are key components. As methods to quantify the severity of inflammation following MI are lacking, we aim to develop in vivo imaging methods to quantify diabetic-enhanced inflammation in infarcted hearts. We intend to use magneto-fluorescent nanoparticles (MFNPs), to assess cardiac function and structure from cardiac cine MRI in healthy, control infarcted, and diabetic infarcted hearts. Ultimately, this research will gain a better understanding of the inflammatory processes occurring in diabetic MI and identify potential therapeutic targets to attenuate adverse cardiac remodeling.

Methods: In this project, *Cx3cr1*$^{GFP/+}$ reporter mice, which express GFP in monocytes and macrophages, were categorized into two groups: (1) control healthy mice, (2) mice that underwent a permanent occlusion of the coronary artery (MI). the investigation of enhanced inflammatory processes following MI. A 9.4 T horizontal MRI scanner with mouse cardiac phased-array surface receive coil (Bruker, Ettlingen, Germany) was used to perform all MRI experiments. A retrospectively gated FLASH sequence (Intragate, Bruker, Ettingen, Germany) was applied to acquire the long axis parameters as end-diastolic volume, end-systolic volume, and infarct size using late gadolinium enhancement were quantified on MRI cine images by matlab-based software.

After MRI experiments, hearts were isolated, rinsed, embedded in paraffin and sectioned. The sections were consequently (a) stained with Masson's trichrome staining to assess the severity of myocardial fibrosis by light microscopy, (b) stained with DAPI to confirm uptake of MFNPs by *Cx3cr1*$^{GFP/+}$ macrophages by fluorescent microscopy. Furthermore, we quantified their intensities in hearts to provide a correlation to inflammatory levels.

Results: The MI group exhibited a statistically significant deterioration in cardiac function compared to the control group. Quantitative analysis demonstrated a higher quantity of nanoparticles within the border zone of the MI group, compared to control healthy myocardial tissue. Although the extent of scar tissue observed through MRI scans and histology slides varied, both methods confirmed the presence of inflammation.

Conclusions: Our results confirm the deleterious effect of LV remodeling on cardiac function and demonstrate the potential use of magneto-fluorescent nanoparticles to quantify and stage inflammation.

Keywords: Myocardial Infarction, Nanoparticles, MRI, Diabetes

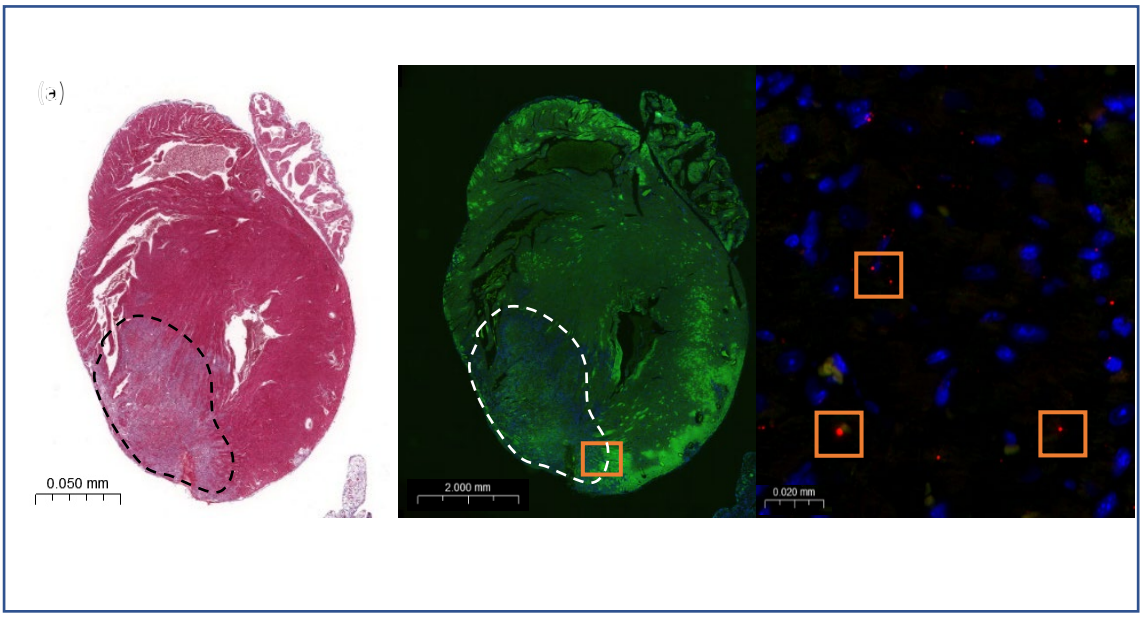

Figure 1: (a) Microscopic image of infarcted heart at day 4 after MI, stained with Masson Trichrome (black dotted line: infarct). (b) Microscopic image of infarcted heart at day 4 after MI (white dotted line: infarct, orange square: infarcted borders). (c) Infarct border area pointing with orange squares at nanoparticles.

26
Fetal EEG: New Born Babies EEG Artifact cleaning and features

Fatma Ebraheem[1], Fauzi Jomaa[1], Zhuo Wang[2], Rotem Shapira[1], and Offer Erez[3]

[1] Faculty of Biomedical Engineering, Technion – ITT, Haifa, Israel
[2] Drexel University School of Biomedical Engineering, Science and Health care
[3] Ben-Gurion University the Joyce and Irving Goldman Medical School

Efforts to study the human fetal electroencephalogram (EEG) have been ongoing since the mid-20th century, driven by the desire to understand fetal brain development, overall health, and detect abnormalities. However, previous approaches to recording and interpreting fetal EEG signals have been limited in their temporal scope and data quality. In this paper, we present a comprehensive analysis of fetal EEG signals using scientific methodologies, aiming to enhance our understanding of their characteristics and explore the potential for non-invasive monitoring throughout human pregnancy.

To achieve accurate and objective analysis of fetal EEG signals, we propose the integration of automated signal processing methods and machine learning techniques. Initially, we employed manual removal of artifacts from neonatal EEG signals as a preprocessing step. Two annotators meticulously identified and marked artifacts, with any disagreements resolved by an expert. This step ensured the elimination of unwanted distortions from the original signals, improving the overall quality and reliability of the data.

Furthermore, our research builds upon previous studies that have established the similarity between EEG signals of newborn babies (aged 0 to 24 hours) and fetal EEG. This knowledge supports the premise that studying neonatal EEG can provide valuable insights into fetal brain activity. By investigating neonatal EEG as a proxy for fetal EEG, we gain access to valuable data that aids in understanding the developmental processes of the fetal brain.

To classify the EEG signals based on their background activity and identify potential abnormal features, we employed advanced machine learning algorithms. These algorithms were trained on labeled data, where experts annotated the EEG signals according to their characteristics. By leveraging the power of machine learning, we were able to automate the classification process and extract meaningful information from the EEG data.

By comparing the results of the original and processed data, we assessed the effectiveness of artifact removal and analyzed the impact on the overall interpretation of the signals. Through this analysis, we gained a deeper understanding of the distinctive characteristics and patterns exhibited by fetal EEG signals, further contributing to our knowledge of fetal brain development.
In our study, we achieved an accuracy of 51.59% and a specificity of 0.81 in classifying fetal EEG signals. These results highlight the efficacy of our approach, combining

automated signal processing methods and machine learning techniques, in accurately analyzing and interpreting the characteristics of fetal brain activity.

Our study demonstrates the feasibility of recording fetal EEG signals with improved accuracy, supporting the potential for non-invasive monitoring throughout the entire duration of human pregnancy. The advancements in signal processing and machine learning techniques allow us to analyze fetal EEG signals in a more objective and efficient manner, paving the way for further research and clinical applications in the field of fetal neurophysiology.

In conclusion, our comprehensive analysis of fetal EEG signals, integrating automated signal processing methods and machine learning techniques, enhances our understanding of their characteristics and provides insights into fetal brain activity. The potential for non-invasive monitoring throughout pregnancy offers new possibilities for assessing fetal health and developmental milestones.

Keywords: fEEG, Neonatal EEG, Neonatal EEG as a proxy for fetal EEG, Artefact removal, cross-validation.

Figure 1 Noisy EEG (in green) vs EEG signal after artefact removal (in yellow)

27

Cancer Cells Detection in Spectral-Imaged Biopsies using Machine Learning

Chen Ziv [1], Daniela Boguslavsky [1], Adam Soker [1] and Yuval Garini [1]

[1] Faculty of Biomedical Engineering, Technion - IIT, Haifa, Israel

Introduction: Cancer diagnostics includes a growing variety of methods ranging from genetic and molecular tests to whole-body imaging. Nevertheless, cancer diagnostics mainly rely on a pathological interpretation of biopsies using traditional glass-slide microscopy of stained tissues and require highly skilled pathologists. The need for diagnosing pathological biopsies is enhanced which requires the procedures to be expedited. As for today, automized diagnosing only exploits the data regarding the color of the biopsies. While analysis and diagnostics using Machine Learning (ML) becomes more common, we are still facing challenges.

Here we are intending to use a spectral imaging optical system. The spectral data is remarkably more informative than the color information and might lead to very high accuracy in identifying cancer cells. By using Different ML techniques and examine the performance of each one, we will be able to automate the process of cancer cells diagnosis.

Methods: First we designed a Graphical User Interface (GUI). This app is used for a Hematoxylin and Eosin (H&E) staining biopsy whose nuclei were segmented in an algorithm that was developed by Adam Soker at Garini's lab. The app was used to add/delete nuclei and mark cancer region based on prelabeled images by pathologists.

Afterwards, we used the labeled images by the GUI and extracted features that can be useful for classifying whether the nucleus is normal or cancerous. Two of the features were calculated based on research that was conducted by Eugene Brozgol at Garini's lab. Those features were calculated using spectral data. The other features were extracted using geometrics properties.

Finally, two different Machine Learning methods were examined: SVM and Decision Trees. The hyper parameters were chosen by cross-validation and the model was trained on a biopsy of one patient. The results were measured using a test set from a biopsy of a different patient and displayed in a truth matrix.

Results: The spectral data is more informative than the color information, and leads to high accuracy in identifying cancer cells, as tested on a random and different cancer case. This was improved even more by adding geometric features that perform good classification on small training set, indicating the high level of information exists in the features that were chosen.

Conclusion: We developed an automated method to classify whether the nucleus is normal or cancerous. This method relays on another automated method - Segmentation. Since our main

goal is to create an automated and expedited procedure for biopsies diagnosing. Through this, we will be able to improve patient care and expedite the treatment procedure.

Key words: Biopsies, Cancer, Automated, Classification

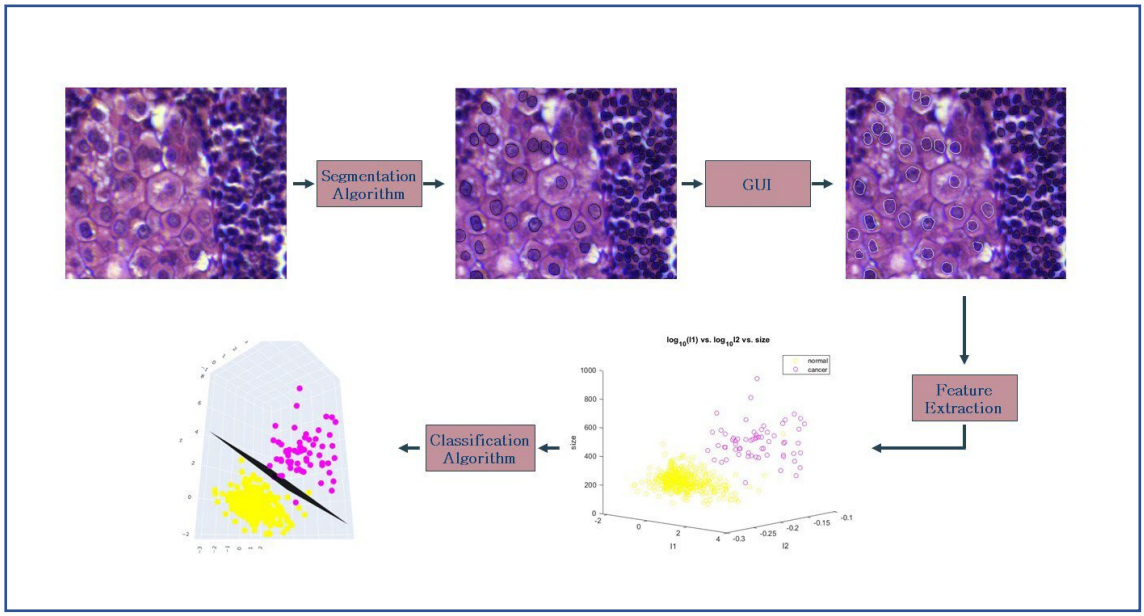

Figure 1: Schematic flowchart of the biopsy analysis process

28

Effects of Microplastic on Alginate Hydrogel Mechanics as a Model for Tissues

Noga Drimer Hocherman[1], Tamar Gil[1], Baptiste Le Roi[2], Merav Belenkovich[1], Oryan Karni Katovich[1], Joshua Grolman[2]

[1]Faculty of Biomedical Engineering, Technion – ITT, Haifa, Israel
[2]Faculty of Materials Engineering, Technion – ITT, Haifa, Israel

The environmental impact of plastic waste is of growing concern. Plastic particles are detected in all ecosystems, and it is one of the main anthropogenic sources of pollution. An average human adult of 70 kg consumes a staggering amount of 0.2-10.2 mg/kg of plastic daily, in the form of microplastic particles (MPP) which are less than 5 mm in length, either purposefully made to be used as exfoliators, or derived via the degradation of other plastic debris.

Plastic has been shown to have a biological effect in simulations and in in *vivo* studies. Specifically, MPP has been shown to accumulate in the organs of mice, and to pose a health risk, in other organisms. Studies have also shown that tissue mechanics can alter cellular behavior and development. Therefore, we seek in this study to uncover how one of the most common types of MPP, polypropylene (PP), affects the mechanics of alginate hydrogels, as tissue models, where cells can later be cultured.

In order to study the effect of particle size we sonicated MPP for 0-60 minutes, and measured their diameter using laser diffraction particle size analyser (dynamic light scattering, DLS). We also immersed the particles in fetal bovine serum (FBS) to coat them and mimic a biological environment, and measured its effect on particle size. We used rheology to quantify the viscoelastic behavior of gels with varying MPP hydrodynamic radii, by applying dynamical shear stress and measuring the gels' storage and loss moduli (G' and G" respectively).

We found that MPP's hydrodynamic radius decreases with sonication duration, reaching a minimum at 30 minutes. Additionally, we found that immersion in FBS nearly doubles particle size, with no significant effect of the FBS concentration. Finally, in the rheology tests we saw that both G' and G" increase with FBS and decrease with sonication, compared with untreated MPP gels.

We conclude that particle size influences the mechanics of alginate gels. An increase in particle size causes an increase in G' and G". We conclude that a biological environment can drive increase in MPP size, and the subsequent change in mechanical properties. In the future, when testing the effect of MPP on live cells, the MPP should be sonicated for 30 minutes or more, in order for the particle size to be controlled.

Keywords: MPP, alginate gels, rheology, sonication, DLS.

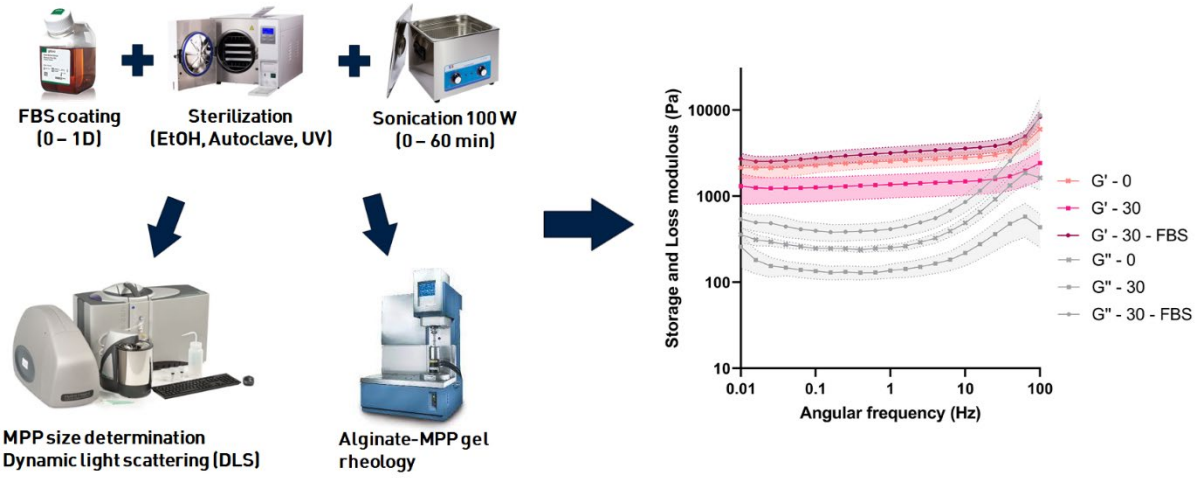

Figure 1: Sonication lowers both G' and G", whereas FBS after sonication raises G' and G".

Left: the experimental process – particles were treated with a combination of the methods at the top, and measured for size using the DLS device and for viscoelastic properties using a rheometer.

Right: results of rheology tests performed on three types of samples, with five replicates each. Each sample was an alginate gel with a concentration of 0.5% MPP: untreated (0), sonicated (30), and immersed in FBS after sonication (30 - FBS).

29

Dynamic Reinforcement Learning Enabled by Virtual Reality

Irina Shkalikov[1], Tamar Ben yaacov[1], Ben Engelhard [2]

[1] Faculty of Biomedical Engineering, Technion - IIT, Haifa, Israel
[2] Engelhard Lab Neural circuits for complex behavior

Introduction: Reinforcement learning, also known as reward-based learning, relies on the regulation of dopamine neurons in the midbrain, particularly in the ventral tegmental area (VTA). This specific brain region plays a crucial role in coordinating various behavioral processes. The dopamine-releasing neurons within the VTA encode the learned connections between stimuli and rewards. They prioritize and guide decision-making to maximize favorable outcomes. However, the ability of this reward system to adapt to rapidly changing environments, where the significance of stimuli and their associations with rewards fluctuate, remains incompletely understood.

To address this gap, we created a VR-based task that alters stimulus significance during the session, that can be further combined with advanced brain imaging to gain new insights into the dopamine system's role in dynamic learning.

Methods: We developed an experimental platform comprising VR software built with Unity and C# coding, along with physical components (spherical treadmill, dynamic virtual T-maze display, and reward-delivering pump) to facilitate a behavioral task (figure 1). Mice are head-fixed under a two-photon microscope to monitor neuronal activity. Utilizing the spherical treadmill, mice perform navigational tasks in the virtual environment, making decisions at the T-maze's end by selecting left or right. Successful choices trigger liquid rewards dispensed by the VR software through the pump. The adaptive T-maze allows for parameter adjustments, gradually training mice from easier to more challenging versions, like "permanent mode", that includes visible stimuli, shorter mazes, and reduced delays. These adaptations were tailored to individual learning progression. The dynamic behavioral task introduces random selection of primary stimulus during trials, facilitating rapid changes in stimulus-reward relationships. Additionally, we adjusted the VR settings to introduce complex tasks and conducted a survey, where participants used a VR game without instructions. The survey aimed to gain insights into user experience and evaluate the learning process.

Results: The modular T-maze was constructed, allowing users to define criteria such as maze period lengths, stimulus types and numbers, permanence mode, and level progression criteria. Implemented input parameters offer flexibility and adaptability, addressing limitations of previous similar software. Each trial starts with a randomly selected main stimulus, followed by cue period stimuli guiding the mouse's turn at the T-junction. Detailed summary files capture stimuli and mouse positions, updating the current level variable for subsequent scenes. Initial survey results are being analysed, and the findings will provide valuable insights.

Conclusions: This study introduces a versatile platform for conducting various behavioral tasks. Future research aims to develop study protocols that adapt task conditions based on individual learning, while analyzing collected data including game records and neuronal signals, to gain insights into learning processes in dynamic environments.

Keywords: Reinforcement learning, stimulus-reward relationship, dynamic task, VR.

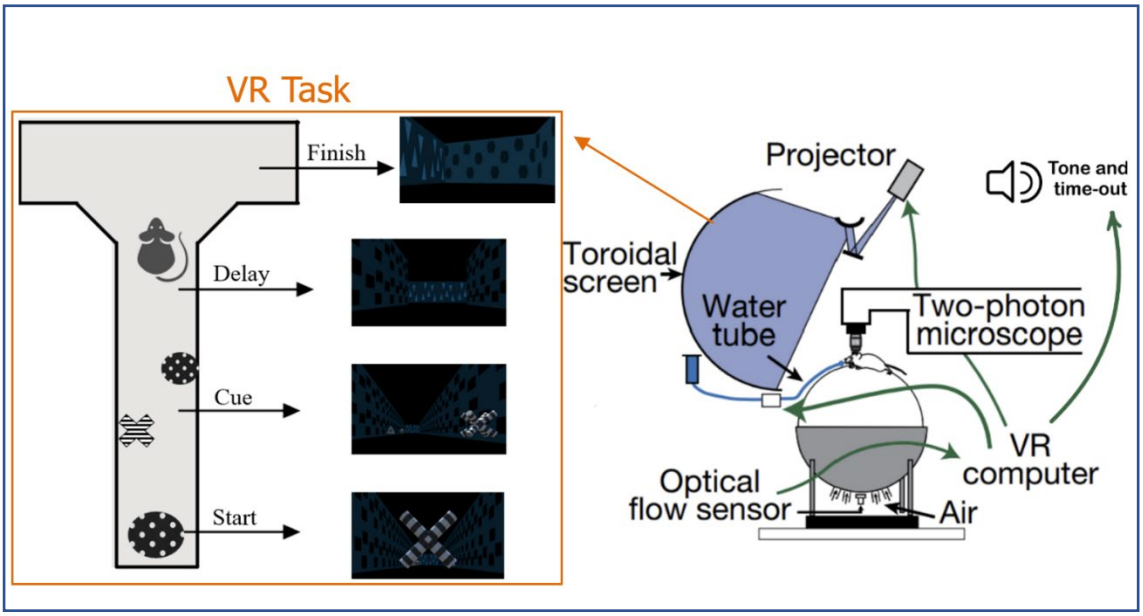

Figure 1: Scheme of the experimental set-up.

30

Decreased Frontal Theta Frequency While Performing a Task With the Existence of Smartphone Among Children: An EEG Study

Rawnaq Shaer[1], Sheherban Nasser Eldin[1], Carmel Gashri[1], Gaia Levin[1], Tzipi Horowitz-Kraus[2]

[1]Faculty of Biomedical Engineering, Technion - IIT, Haifa, Israel
[2]Faculty of Education in Science and Technology – IIT, Haifa, Israel

Introduction: Smart devices have become an integral part of our daily lives, transforming the way we communicate and access information. However, research has highlighted the potential implications of smartphone presence on task performance, particularly in young children. Cognitive interruptions were previously characterized by changes in frontal theta (4-8 Hz) and alpha (8-13 Hz) frequencies measured using Electroencephalography (EEG). To gain a deeper understanding of this phenomenon, we conducted a comprehensive study using EEG to detect brain patterns associated with smartphone presence in children.

Methods: During the study, EEG data were collected from 5.3-8.5-year-old children performing a simple reaction time task. The same experiment was conducted twice, once with the presence of a smartphone and once without. Theta and alpha bands were calculated from 5 frontal electrodes (FP1, FP2, F7, F8, Fz). By analyzing the collected EEG data using signal processing software and statistical methods, we aimed to identify specific brain patterns linked to the presence of smartphones during task performance. A 2 x2 repeated measure analysis of variance (ANOVA) was performed to assess the impact of two conditions on alpha and theta bands: 1)with the presence of a smartphone and; 2) without the presence of a smartphone. Additionally, the EEG measures were correlated with standardized cognitive measures evaluating attention abilities derived from the Test of Everyday Attention (TEA-CH) using Pearson correlation.

Results: The analysis of the EEG data revealed a significant main effect of frequency, with theta frequencies showing greater activity compared to alpha frequency. Additionally, a trend of main effect of condition was found (theta and alpha activity was higher in the absence of a smartphone compared to its presence), with a significant difference between theta bands for the two study conditions using paired t-test. Moreover, the differences between alpha and theta bands in the two conditions were significantly correlated with lower scores of auditory and visual attention and inhibition tests. These findings suggest that the existence of an interactive electronic device during cognitive tasks is associated with alterations in brain activity related to cognitive control.

Conclusions: These findings have important implications for future research, regulatory decisions, and initiatives aimed at promoting safe smartphone use in young children. By identifying distinct brain patterns associated with smartphone interference, we shed light on the neurological mechanisms underlying changes in task performance. This knowledge can inform the development of strategies to optimize cognitive function and minimize potential adverse effects in young children.

Keywords: Smartphone interference, Electroencephalography (EEG) , Children, Neural functioning.

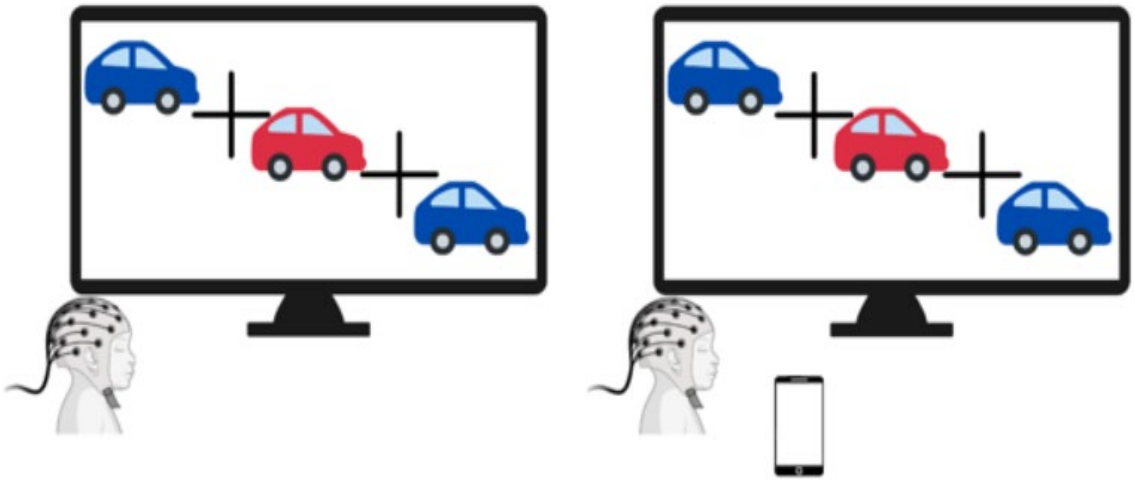

Figure 1: An illustration of the Simple Reaction Time task: left: the condition without the existence of a smartphone; right: the condition with the existence of a smartphone

31

Developing a Non-Invasive Imaging Platforms to Genetically Track Hematopoietic Stem and Progenitor Cells and Their Offspring During Inflammation

Mira Waked[1], Liron-Hanan Waingerten-Kedem[1], Shiri Ashkenazi[1], Katrien Vandoorne[1]

[1]Faculty of Biomedical Engineering, Technion - IIT, Haifa, Israel

Introduction: Bone marrow hematopoietic stem and progenitor cells are cells within the bone marrow that throughout life replenish all lineages of blood cells. During episodes of inflammation in the body, the hematopoietic stem cells (over) produce inflammatory myeloid cells, their engraftment and dynamics have been previously genetically monitored by bioluminescence imaging, but their genetic labeling has not yet been employed for visualizing inflammatory changes at the bone marrow. Our goal is to develop magnetic resonance reporter gene methods to image the dynamics of hematopoietic stem cells, in particular Lineage-Sca-1+c-Kit+ (LSK) cells, at the bone marrow and in the future, follow the release and production of inflammatory myeloid cells during inflammation.

Methods: For isolating LSKs, murine bone marrow cells were pooled to obtain enough LSKs for transfection by (a) non-stem cell lineage depletion and (b) sorting LSKs. The marrow of the bones was collected by flushing. (a) Isolated bone marrow cells were stained with biotin conjugated antibodies against lineage markers, followed by anti-biotin monoclonal antibodies conjugated to MicroBeads. The magnetically labeled Lin^+ cells were depleted by their retention to the MACS Columns. After depletion, cells were stained with streptavidin BV605 conjugates and antibodies against cKit anti-Sca-1 to identify efficiency of the depletion and isolate LSKs using flow cytometry cell sorting. After sort, LSKs were cultured in StemPro™-34SFM medium. For cell transfection (2), Escherichia coli was inoculated with the transfected plasmid, namely pLentipuro3/TO/V5-GW/EGFP-Firefly Luciferase, which incorporates our reporter gene luciferase. The bacterial culture was then cultivated to facilitate the generation of lentiviral vectors. Subsequently, the plasmid DNA was purified using the Midiprep kit, followed by elution of the purified plasmid DNA. The final step involved cellular imaging using in Vivo Imaging System (IVIS). The objective was to evaluate the sensitivity of cells (4T1 cells), expressing a luciferase containing plasmid, quantifying the emitted bioluminescence during the reaction with luciferin catalyzed by firefly luciferase

Results: We successfully isolated LSK cells by depletion combined with flow cytometric sorting. The LSK population comprised 0.5% of the total bone marrow cells. This number of LSKs allowed us to culture them. Following plasmid DNA elution, we confirmed the quality and presence of luciferase by subjecting it to sequencing analysis. As a proof-of-concept, to verify the efficiency of IVIS bioluminescence imaging of cells, we successfully detected and quantified bioluminescent signals emitted by cells.

Conclusions: We successfully sorted LSKs and cultured them. Moreover, we demonstrated the efficacy of Luciferase in facilitating IVIS imaging. In the future, the infection of LSK cells will need to be optimized and quantification of IVIS imaging for LSK cells that contain our plasmid will need to be established.

Keywords: plasmid, bioluminescence, LSK

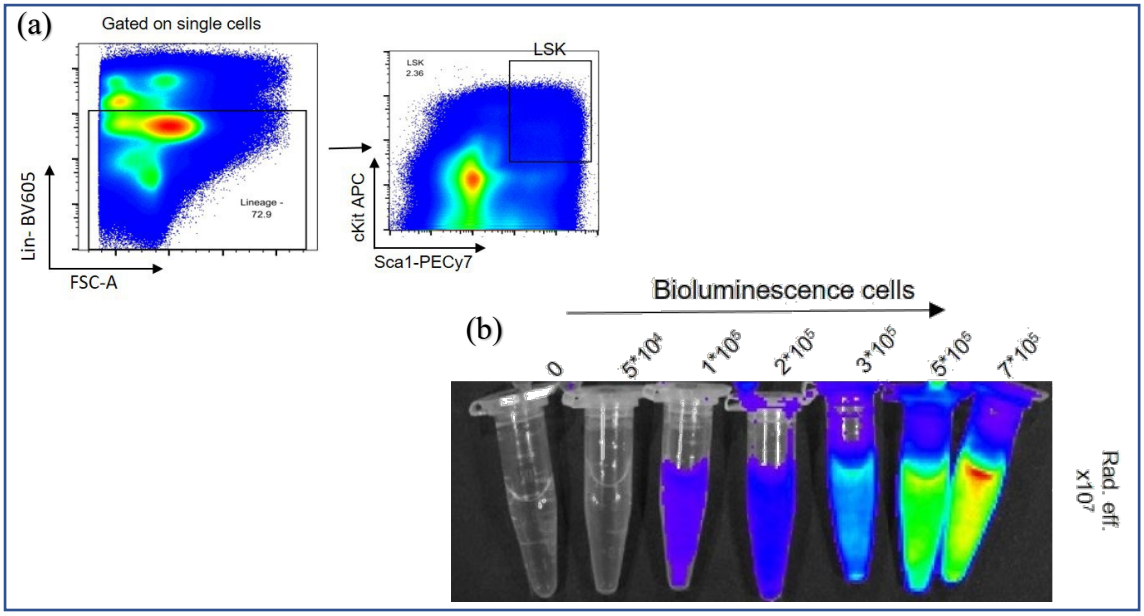

Figure 1: LSK cells sorting and bioluminescence imaging by IVIS. (a) Flow cytometric gating for LSKs (b) IVIS imaging 4T1 Cells that have luciferase containing plasmid.

32

Reducing the electrocardiogram time series lead system for arrhythmia diagnosis and age estimation tasks

Shahar Rashty[1], Sarah Teitz[1], Rotem Shapira[1], Eran Zvuloni[1] and Joachim Behar[1]

[1] Faculty of Biomedical Engineering, Technion - IIT, Haifa, Israel

Introduction: The 12-lead electrocardiogram (ECG) is a standard tool used in medical practice for identifying cardiac pathologies. Its acquisition requires 10 electrodes and is usually performed for a short period of time. Recording, acquiring, and interpreting the full 12-lead system requires professional expertise or computational resources that are not readily available in all medical institutions or in large areas of developing countries.

Previous studies have performed several ECG tasks using a reduced lead set, which was either predefined or was reduced from the original set by applying principal component analysis (PCA). Although these studies showed the feasibility of using reduced lead systems, these were confined to a specific domain knowledge, or had not shown a general approach that serves various of ECG analysis tasks.

Here, we introduce a new deep-learning-based approach to produce the reduced lead set. The pipeline can be applied for any ECG analysis task at hand. We demonstrate our approach by performing both six cardiac arrhythmia diagnosis and patient age estimation tasks.

Methods: The PTB-XL dataset was used, including 21,837 12-lead ECG recordings from 18,885 patients. State-of-the-art (SOTA) models for arrhythmia diagnosis (multi-label classification) and age estimation (regression) were modified to obtain the 12-lead ECG baseline performance. Next, for selecting the reduced lead system, another ECG analysis model was used to extract lead-specific features and linearly combines them. This enabled to utilize a recursive lead elimination (RLE) technique, which eliminated less significant leads in an iterative manner, and validating the model performance for each elimination step. Last, the baseline performance was reproduced with the SOTA models using the reduced lead set. Performance was measured using the area under the precision recall curve (AUPRC) and the mean absolute error (MAE) for the classification and regression tasks, respectively.

Results: Baseline test performance obtained a mean AUPRC=0.64 and MAE=8.39. By applying the RLE, we are able to maintain test set performance of mean ΔAUPRC=0.062 and ΔMAE=-7.74 (Fig. 1), while eliminating V_5, V_4, V_6, V_3 and I, V_4, V_2, V_1 respectively.

Discussion and conclusion: A reduced lead system of 8 leads was able to reproduce the full 12-lead system results for the classification task and the age estimation tasks. Although, both reduced lead systems have an equal number of leads, they consist of different leads. Thus, our proposed technique demonstrated its applicability for any specific task-dependent lead systems.

Keywords: ECG, reduced lead system, arrythmia, age estimation, recursive feature elimination

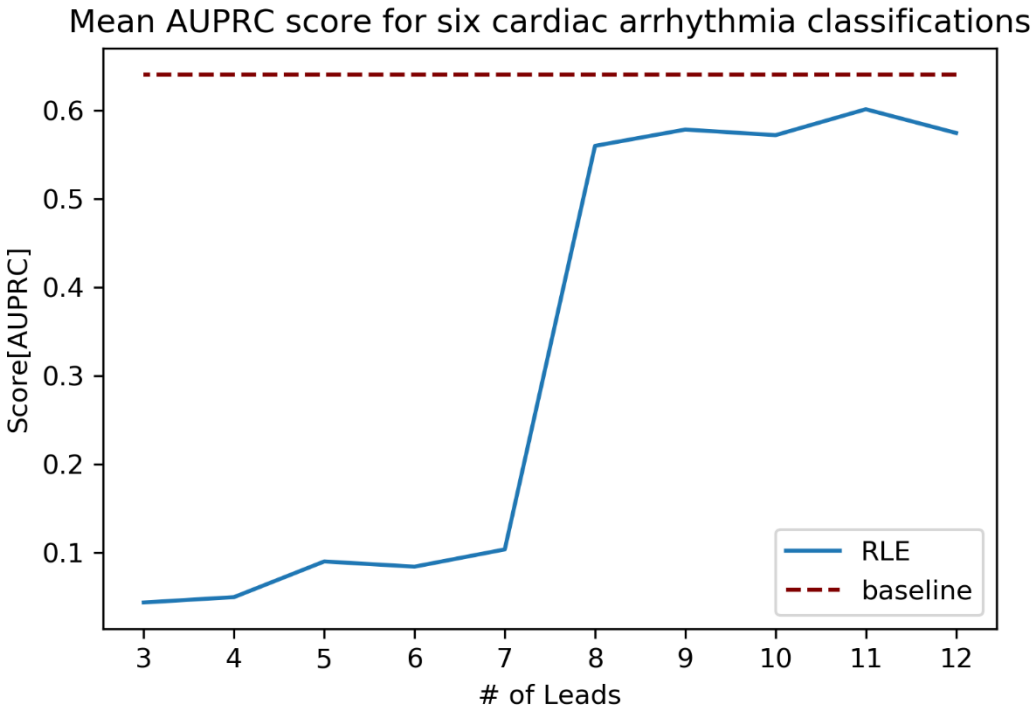

Figure 1: RLE result for the six arrhythmia diagnosis classification task. Test set mean AUPRC score for six cardiac arrhythmias (1st degree AV block, right bundle branch block, left bundle branch block, sinus bradycardia, atrial fibrillation, and sinus tachycardia) as a function of the number of leads in the reduced ECG lead set.


BME